ACS Chemical Neuroscience

pubs.acs.org/chemneuro Research Article

Phenothiazine-Tacrine Heterodimers: Pursuing Multitarget Directed Approach in Alzheimer's Disease

Lukas Gorecki, Elisa Uliassi, Manuela Bartolini, Jana Janockova, Martina Hrabinova, Vendula Hepnarova, Lukas Prchal, Lubica Muckova, Jaroslav Pejchal, Jana Z. Karasova, Eva Mezeiova, Marketa Benkova, Tereza Kobrlova, Ondrej Soukup, Sabrina Petralla, Barbara Monti, Jan Korabecny,* and Maria Laura Bolognesi*

Cite This: ACS Chem. Neurosci. 2021, 12, 1698−1715 Read Online

ACCESS | Metrics & More | Article Recommendations | Supporting Information

ABSTRACT: Since 2002, no clinical candidate against Alzheimer's disease has reached the market; hence, an effective therapy is urgently needed. We followed the so-called "multitarget directed ligand" approach and designed 36 novel tacrine-phenothiazine heterodimers which were *in vitro* evaluated for their anticholinesterase properties. The assessment of the structure−activity relationships of such derivatives highlighted compound **1dC** as a potent and selective acetylcholinesterase inhibitor with IC_{50} = 8 nM and **1aA** as a potent butyrylcholinesterase inhibitor with IC_{50} = 15 nM. Selected hybrids, namely, **1aC**, **1bC**, **1cC**, **1dC**, and **2dC**, showed a significant inhibitory activity toward $\tau_{(306-336)}$ peptide aggregation with percent inhibition ranging from 50.5 to 62.1%. Likewise, **1dC** and **2dC** exerted a remarkable ability to inhibit self-induced $A\beta_{1-42}$ aggregation. Notwithstanding, *in vitro* studies displayed cytotoxicity toward HepG2 cells and cerebellar granule neurons; no pathophysiological abnormality was observed when **1dC** was administered to mice at 14 mg/kg (i.p.). **1dC** was also able to permeate to the CNS as shown by *in vitro* and *in vivo* models. The maximum brain concentration was close to the IC_{50} value for acetylcholinesterase inhibition with a relatively slow elimination half-time. **1dC** showed an acceptable safety and good pharmacokinetic properties and a multifunctional biological profile.

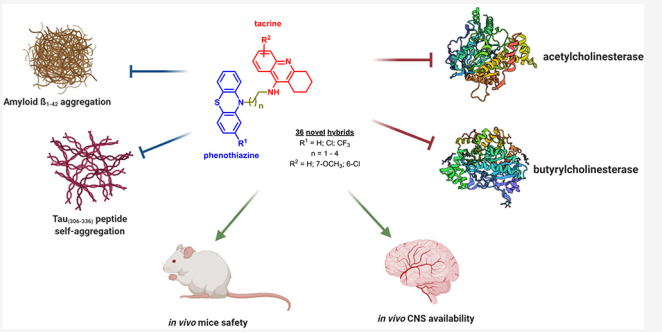

KEYWORDS: *Alzheimer's disease, acetylcholinesterase, butyrylcholinesterase, phenothiazine, tacrine, multitarget directed ligands*

INTRODUCTION

The etiology of Alzheimer's disease (AD) comprises intertwined mechanistic pathways which, for an effective therapeutic intervention, might be better addressed by a multitarget approach.[1,2] This builds upon the fact that several targets can be simultaneously modulated by a single small molecule, i.e., a multitargeted directed ligand (MTDL).[1] Developing MTDLs has represented a challenging task for many researchers around the world in the past couple of decades.[3,4] Although reaching some preclinical successes, none of the developed MTDLs have been approved yet for the treatment of neurodegenerative diseases including AD.[5] Because different hypotheses of AD pathophysiology have been postulated, the appropriate target selection for the MTDL design is a matter of crucial importance.[6,7]

The so-called cholinergic hypothesis first attempted to explain the pathophysiological processes behind the AD.[8] Currently, cholinesterase inhibitors such as donepezil, galantamine, and rivastigmine are still one of the only two therapeutic options to temporarily improve cognitive function and memory in AD patients.[9] Amyloid plaques[10,11] and neurofibrillary tangles composed of hyperphosphorylated τ protein[12,13] are the two major AD hallmarks. Thus, several AD drug discovery programs have attempted to address these two targets, and first-in-class MTDLs have been developed for this purpose.[14,15] In addition, several other hypotheses have emerged in recent years like those pointing to glutamate excitotoxicity,[16] oxidative stress,[17] and biometal dyshomeostasis[18] as causative triggers of the underlying neurodegeneration. However, the impressive amount of knowledge regarding novel acetylcholinesterase (AChE) functions, as well as the close association between the cholinergic system and other key elements for AD pathogenesis, accounts for the fact that the

Received: March 26, 2021
Accepted: April 7, 2021
Published: April 14, 2021

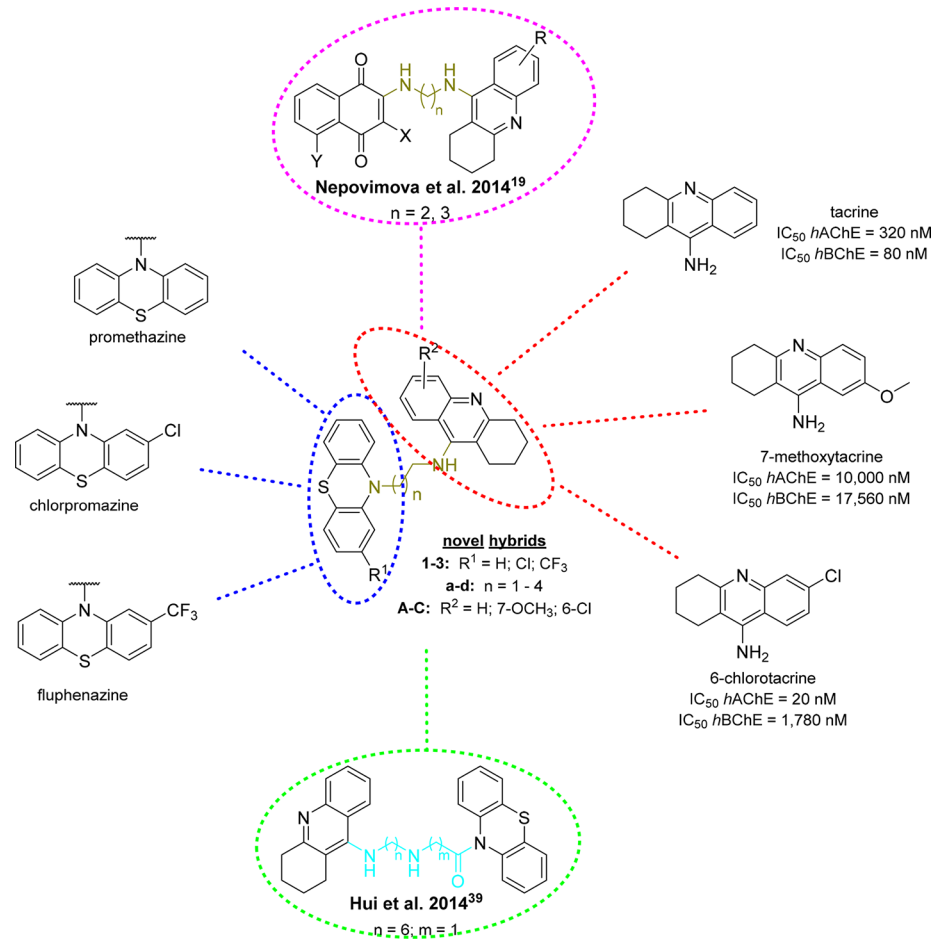

Figure 1. Design strategy for tacrine-PHTs **1−3(a−d)A−C**. General structures for highly efficient naphthoquinone-tacrine derivatives (in pink-dashed line)[20] and for previously reported tacrine-PHTs (in green-dashed line) are outlined.[40]

development of multitarget cholinesterase inhibitors still has great potential.[19]

On these bases, we envisaged novel MTDLs by combining tacrine and phenothiazine (PHT) scaffolds (Figure 1). In detail, we were motivated by the promising results obtained for tacrine-naphthoquinone heterodimers linked through an alkylenediamine spacer (Figure 1), which were endowed with anticholinesterase, antiaggregating and antioxidant features, and a lower hepatotoxicity.[20] Thus, following a similar rationale, we sought to combine the antiaggregating and antioxidant properties of the phenothiazine (PHT) core (see below) to the anticholinesterase effect of tacrine scaffold. Note that tacrine was the first marketed therapeutic agent for the AD treatment as a dual inhibitor of AChE/butyrylcholinesterase (BChE) enzymes.[21] Upon tacrine withdrawal due to severe hepatotoxicity, 7-methoxytacrine (7-MEOTA) and 6-chlorotacrine emerged as the result of an intensive follow-up research in finding more potent (6-chlorotacrine) and less toxic (7-MEOTA) drug candidates.[22,23]

PHT is a tricyclic motif recurring in several drugs for neurological disorders, including promethazine for preoperative sedation or chlorpromazine for schizophrenia treatment.[24,25] The PHT-based drugs chlorpromazine and fluphenazine are listed in the so-called "List of Essential Medicines 2017 (WHO)" for the treatment of psychotic disorders.[24,26] Interestingly, chlorpromazine has displayed neuroprotective effects by protecting mitochondria and preventing apoptosis and by promoting neuronal regeneration and survival.[27,28] PHTs also possess a strong antioxidant capacity.[29,30] We recently proposed a PHT-alkylamine as a privileged chemotype against neurodegeneration.[31] Moreover, BChE inhibitory activity and selectivity over AChE of several PHT derivatives has already been reported.[32,33] In addition, some of these drugs, including the well-known PHT dye methylene blue (MB), were found to be effective inhibitors of amyloid-β peptide (Aβ) aggregation[34] and τ filament formation.[34] MB emerged as a promising AD drug following the successful results of a phase II clinical trial performed with mild-to-moderate AD patients by TauRx Pharmaceuticals Ltd.[35] In spite of these results and good outcomes from *in vivo* studies on animal models, leuco-methylthioninium-bis(hydromethanesulfonate), a derivative of MB, failed to slow down AD progression in the phase III clinical trial.[34,36−38] However, this negative conclusion might be the result of a weak study design and statistical methodology, in addition to the lack of a proper placebo group.[39]

Collectively, it could be envisaged that MTDLs designed by combining tacrine and PHT scaffolds could bring interesting insights into AD treatment. The first attempt to link unsubstituted tacrine and PHT cores was made in 2014 by Hui et al. (Figure 1).[40] However, only three compounds (with PHT-alkylamide structures) were synthesized and assayed on rat brain homogenate for their AChE inhibitory activity. They were further evaluated on okadaic-acid-induced phospho-τ

https://doi.org/10.1021/acschemneuro.1c00184
ACS Chem. Neurosci. 2021, 12, 1698−1715

accumulation in N2α cells. The lead compound (1-(10*H*-phenothiazin-10-yl)-2-({6-[(1,2,3,4-tetrahydroacridin-9-yl)-amino]hexyl}amino)ethan-1-one) was advanced for its ability to bind Aβ_{1-40} fibrils as determined by a surface plasmon resonance sensing assay. Overall, in addition to being a 89 nM potent inhibitor of rat AChE from rat brain homogenate, it proved to be effective in preventing τ phosphorylation and showed to be able to bind Aβ fibrils.[40]

In contrast and within this study, we significantly broadened the library of tested compounds while preserving the phenothiazine-alkylamine fragment. We expanded the chemical space by exploring methylene linkers of different lengths (ranging from 2 to 5 methylenes) connecting the two pharmacophores (**a-d** letters denote the length of the linker ranging from 2 to 5 carbons and designate the final structures). This length of the tether has been shown to impact AChE/BChE recognition. More specifically, the shortest linker should yield BChE selectivity, while 3- and 4-methylene linkers should result in nonselective inhibitors; finally, the five-methylene linker might impose AChE preference.[6,41−43] Furthermore, tacrine-PHT derivatives reported herein are based on three different tacrine fragments (**A**, **B**, and **C** for tacrine, 7-methoxytacrine (7-MEOTA), and 6-chlorotacrine, respectively), with different activities and toxicity profiles. In addition, variously substituted PHT cores were explored (**1**, **2**, and **3** for PHT, 2-chlorophenothiazine, and 3-trifluoromethylphenothiazine, respectively), enabling the formation of 36 tacrine-PHTs (**1−3(a−d)A−C**; Figure 1). Herein, we describe their synthesis and *in vitro* evaluation, as well as the assessment of the preliminary *in vivo* profile. Initially, cholinesterase activity was assayed to draw structure−activity relationships (SARs). The effect of PHT moieties on biological activity was then evaluated by measuring antioxidant capacity, inhibition of $\tau_{(306-336)}$ peptide aggregation and inhibition of self-induced Aβ_{1-42} aggregation. Cytotoxicity and *in vivo* safety, together with *in vitro* BBB penetration of selected hybrids, were investigated.

RESULTS AND DISCUSSION

Chemistry. The synthetic route for tacrine-PHTs **1−3(a−d)A−C** started with the formation of the acetals **6**, **7**, **10**, and **12** (Scheme 1). These reactions were carried out as previously described (see Supporting Information, Schemes S1 and S2).[31,44] Aldehyde **9** was prepared according to Jackson et al.[45] and converted to acetal **10** by triethyl orthoformate treatment. Once the acetal intermediates were synthesized, the subsequent reductive amination of **13−15** yielded the amide derivatives of PHT (**16−27**; Scheme 2).[46] The subsequent hydrolysis of amides **16−27** enabled amine formation (**28−39**; Scheme 2) under three different procedures. In particular, the trifluoroacetamide protecting group of **16−21** was removed under mild conditions (K_2CO_3) leading to the primary amines **28−33**. Compounds **22−24** bearing an acetamide group were hydrolyzed using KOH under microwave (MW) irradiation allowing formation of **34−36**. To obtain primary amines **37−39**, deprotection of phthalimides **25−27** was carried out using hydrazine hydrate. Finally, primary amines **28−39** were utilized as key starting material for the formation of the final products **1−3(a−d)A−C** by reaction with 9-chloro-1,2,3,4-tetrahydroacridine derivatives **A−C** in phenol under MW irradiation (Scheme 3).[47]

Scheme 1. Preparation of Selected Acetals 6, 7, 10, and 12[a]

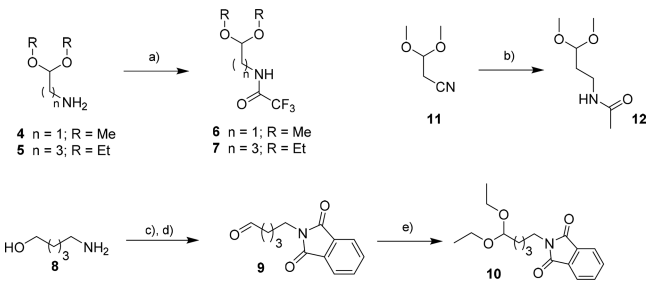

[a]Reagents and conditions: (a) TFAA, TEA, THF, 0 °C to RT; (b) Ac_2O, $NiSO_4$, $NaBH_4$, MeOH, 0 °C to RT; (c) phthalic anhydride, 150 °C; (d) $(COCl)_2$, DMSO, DIPEA, DCM, −45 °C to RT; (e) TsOH, triethyl orthoformate, EtOH, RT.

Cholinesterases Inhibitory Activity. The inhibition of both human AChE (*h*AChE) and human BChE (*h*BChE) by **1−3(a−d)A−C** was evaluated by a modified Ellman method.[48] Results (Table 1) confirmed that all the compounds were potent cholinesterase inhibitors. Compounds displayed anti-cholinesterase activity spanning from the micromolar to nanomolar scales (nanomolar activity was displayed by derivatives **1dA**, **1dC**, and **2dC** for *h*AChE; **1aA**, **1aC**, **2aA**, **2aC**, **3aA**, **1cA−C**, **1dA**, **2dA**, and **3dA** for *h*BChE) and showed a clear influence by substituents and linkers. In detail, strong inhibitory activity toward *h*AChE was obtained for compounds bearing a five-methylene tether (**1−3dA** or **1−3dC**), with the exception of 7-MEOTA-based heterodimers **1dB**, **2dB**, and **3dB**. In contrast, compounds bearing the shortest two-carbon linker (**1−3aA-C**) were the most potent toward *h*BChE. Similar results have been already reported for other heterodimers/homodimers such as bis-tacrines or tacrine-based MTDLs with different linkers.[6,41,42,49] It might be inferred that the chain length is important to properly accommodate the PHT nucleus which, being bulky and rigid, may generate some steric clashes. When the chain length is composed by four or five carbon atoms, the PHT moiety presumably better approaches the peripheral anionic site at the mouth of *h*AChE. This enhances the selectivity and affinity toward this enzyme. Conversely, because the gorge of *h*BChE is shorter and nearly double in size compared to that of *h*AChE,[50] the interaction of tacrine-PHTs featuring a shorter alkylene chain is favored. Hence, for hybrids with shorter linkers, selectivity is shifted toward *h*BChE.[50,51] Generally, most active derivatives toward *h*BChE and *h*AChE bear a two-methylene (**1−3aA−C**) and five-methylene (**1−3dA-C**) chain, respectively. In agreement with the higher inhibitory potency of 6-chlorotacrine vs tacrine on *h*AChE, the derivatives bearing such a fragment (**1−3(a−d)C**) were more potent (IC_{50} = 8−1500 nM) than tacrine analogues (**1−3(a−d)A**; IC_{50} = 0.08−13.1 μM). Similarly, those bearing a 7-MEOTA fragment (**1−3(a−d)B**) were the least potent against *h*AChE enzyme (IC_{50} > 0.6 μM). No clear SAR could be drawn for PHT moiety when dealing with *h*AChE inhibition. Only 2-trifluoromethyl (**3(a−d)A−C**) derivatives appeared to be slightly less efficient than the 2-chloro- (**2(a−d)A−C**) or unsubstituted PHTs (**1(a−d)A−C**). The *h*BChE activity is improved in subsets with 2-trifluoromethyl (**3(a−d)A−C**) and diminishes in 2-chloro derivatives (**2(a−d)A−C**) followed by unsubstituted PHTs (**1(a−d)A−C**). **1dC** was highlighted as the best inhibitor of *h*AChE (IC_{50} = 8 nM) with a selectivity index toward *h*AChE of 24. In addition, **1aA** was selected as the best

https://doi.org/10.1021/acschemneuro.1c00184
ACS Chem. Neurosci. 2021, 12, 1698−1715

Scheme 2. Reductive Amination for Preparation of *N*-Protected-ω-aminoalkylenephenothiazine Derivatives 16−27 and Their Subsequent Deprotection[a]

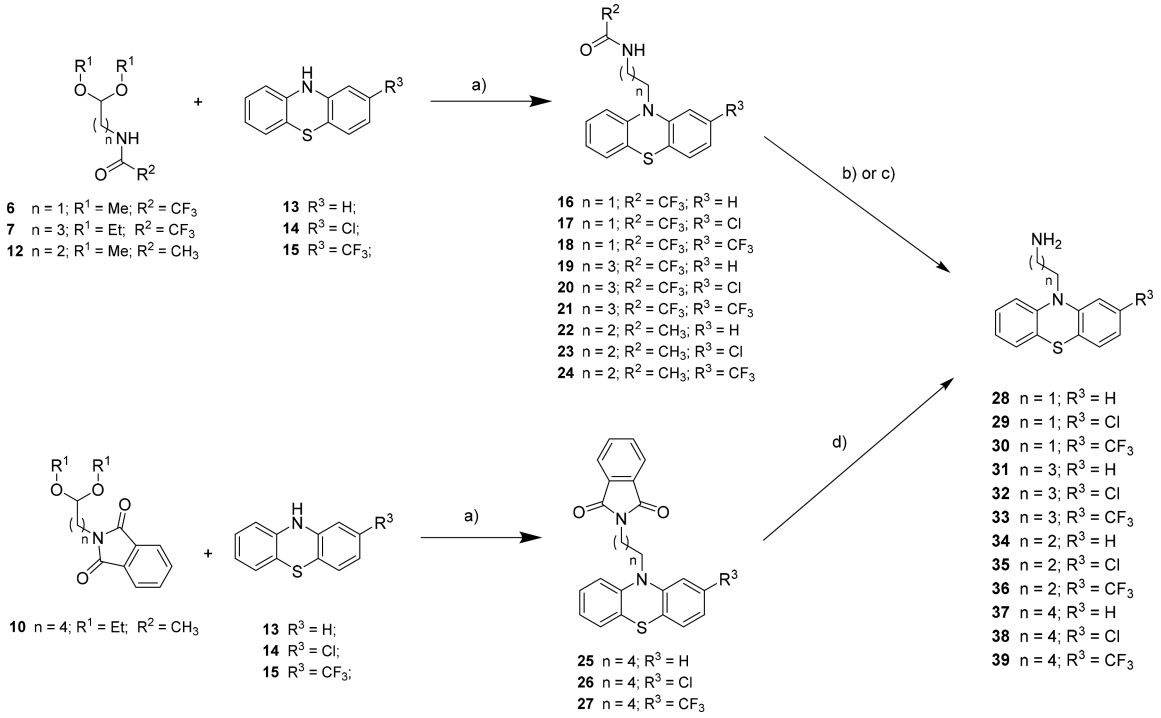

[a]Using (b) conditions for trifluoroacetamide compounds **16−21**, (c) conditions for compounds **22−24** with acetamide group, and (d) conditions for phthalimides **25−27**. Reagents and conditions: (a) TFA, TES, DCM, RT; (b) K_2CO_3, MeOH/H_2O (2:1), RT; (c) MW, KOH, 160 °C, MeOH/H_2O (2:1); (d) $NH_2NH_2{\cdot}H_2O$; EtOH; 90 °C.

Scheme 3. Final Step Leading to the Desired Hybrids 1−3(a−d)A−C[a]

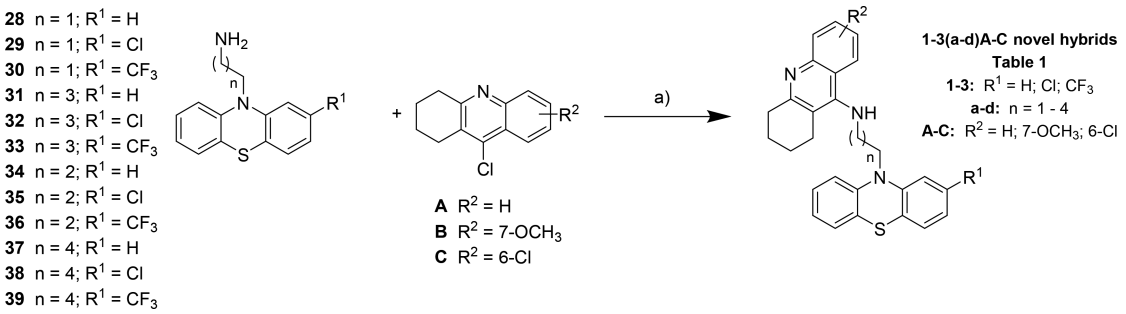

[a]Reagents and conditions: (a) MW, 180 °C, phenol.

*h*BChE inhibitor (IC_{50} = 19 nM) with a selectivity index toward *h*BChE around 100.

Both cholinesterases are distributed within the brain areas (hippocampus, temporal neocortex, and amygdala)[52,53] connected with memory functions, speech creation, and recall of memories. However, while AChE is mostly localized in the synaptic cleft between neurons, BChE is mainly found in the glial cells. Alterations in AChE and BChE expression occur in AD.[54] AChE plays a predominant role in the brain of healthy subjects, in which it acts as the main actor in the hydrolysis of the neurotransmitter acetylcholine (ACh); however, AChE activity decreases with the progression of AD. BChE is able to hydrolyze ACh and can compensate for AChE when its levels are lowered. It has also been reported that BChE might slow down the formation of neurotoxic Aβ fibrils *in vitro*.[55] However, the connection between BChE and Aβ fibrils/amyloid plaques remains quite controversial. On one hand, researchers showed that some variants of BChE are able to attenuate amyloid fibril formation *in vitro*;[56,57] on the other hand, recent *in vivo* experiments demonstrated that BChE may play a role in AD plaque maturation.[58] For the above-mentioned reasons, the hypothesis that BChE-selective or BChE-nonselective inhibitors are more efficient in preventing amyloid aggregation cannot be unequivocally postulated.

A kinetic study was performed to determine the inhibition mechanism of compounds **1dA** and **1dC**, selected on the basis of the most pronounced cholinesterase inhibition properties. Inhibition kinetics were elucidated from velocity curves which were measured at several concentrations of tested compounds and substrate. The type of enzyme inhibition and kinetic parameters (K_i and K_i') were determined using nonlinear regression analysis. Results for each type of model of inhibition (competitive, noncompetitive, uncompetitive, and mixed) were compared by the sum-of-squares *F*-test. Statistical analysis

https://doi.org/10.1021/acschemneuro.1c00184
ACS Chem. Neurosci. 2021, 12, 1698−1715

Table 1. Inhibitory Activity of 1−3(a−d)A−C against *h*AChE and *h*BChE with Calculated Selectivity Index for *h*AChE

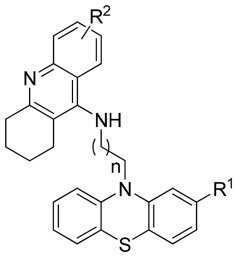

1-3(a-d)A-C novel hybrids
1: R^1 = H; **2**: R^1 = Cl; **3**: R^1 = CF_3
a: n = 1; **b**: n = 2; **c**: n = 3; **d**: n = 4
A: R^2 = H; **B**: R^2 = 7-OCH_3; **C**: R^2 = 6-Cl

compound	n	R^1	R^2	IC_{50} *h*AChE (nM) ± SEM[a]	IC_{50} *h*BChE (nM) ± SEM[a]	selectivity index *h*AChE[b]
1aA	1	H	H	2040 ± 80	19 ± 1	0.01
1aB	1	H	7-OCH_3	4040 ± 310	120 ± 2	0.03
1aC	1	H	6-Cl	280 ± 10	26 ± 1	0.09
2aA	1	Cl	H	1210 ± 30	51 ± 1	0.04
2aB	1	Cl	7-OCH_3	9010 ± 840	140 ± 3	0.01
2aC	1	Cl	6-Cl	350 ± 20	85 ± 3	0.24
3aA	1	−CF_3	H	1710 ± 110	69 ± 4	0.04
3aB	1	−CF_3	7-OCH_3	18 600 ± 2700	480 ± 10	0.03
3aC	1	−CF_3	6-Cl	370 ± 20	300 ± 7	0.83
1bA	2	H	H	4520 ± 380	120 ± 4	0.03
1bB	2	H	7-OCH_3	3500 ± 200	400 ± 10	0.11
1bC	2	H	6-Cl	320 ± 10	260 ± 10	0.81
2bA	2	Cl	H	830 ± 80	210 ± 5	0.25
2bB	2	Cl	7-OCH_3	590 ± 20	810 ± 20	1.37
2bC	2	Cl	6-Cl	260 ± 20	950 ± 30	3.7
3bA	2	−CF_3	H	1700 ± 110	230 ± 10	0.14
3bB	2	−CF_3	7-OCH_3	5840 ± 30	1850 ± 50	0.32
3bC	2	−CF_3	6-Cl	450 ± 20	1040 ± 30	2.3
1cA	3	H	H	4690 ± 540	92 ± 4	0.02
1cB	3	H	7-OCH_3	6330 ± 500	47 ± 3	0.01
1cC	3	H	6-Cl	440 ± 30	66 ± 2	0.15
2cA	3	Cl	H	1820 ± 110	150 ± 2	0.08
2cB	3	Cl	7-OCH_3	2830 ± 250	130 ± 3	0.05
2cC	3	Cl	6-Cl	480 ± 40	230 ± 8	0.48
3cA	3	−CF_3	H	13 100 ± 800	430 ± 13	0.03
3cB	3	−CF_3	7-OCH_3	24 100 ± 3400	580 ± 20	0.02
3cC	3	−CF_3	6-Cl	1450 ± 150	3820 ± 800	2.6
1dA	4	H	H	84 ± 2	19 ± 1	0.23
1dB	4	H	7-OCH_3	>100 000	830 ± 30	>0.01
1dC	4	H	6-Cl	8 ± 0.4	190 ± 10	23.8
2dA	4	Cl	H	330 ± 20	34 ± 1.0	0.10
2dB	4	Cl	7-OCH_3	>100 000	810 ± 30	>0.01
2dC	4	Cl	6-Cl	29 ± 2	420 ± 20	14.5
3dA	4	−CF_3	H	720 ± 50	81 ± 2	0.11
2dB	4	−CF_3	7-OCH_3	>100 000	2350 ± 90	>0.02
3dC	4	−CF_3	6-Cl	120 ± 10	4350 ± 130	36.3
tacrine[c]				320 ± 13	80 ± 1	0.28
7-MEOTA[c]				10 000 ± 974	17 560 ± 795	1.8
6-chlorotacrine[c]				20 ± 1	1780 ± 97	115
donepezil[d]				12 ± 2	7273 ± 621	606

[a]The results are expressed as the mean of at least three experiments. [b]Selectivity for *h*AChE is determined as the ratio of *h*BChE IC_{50}/*h*AChE IC_{50}; [c]Data taken from ref 49. [d]Data taken from ref 42.

showed a mixed-type mode of inhibition with *h*AChE for **1dC** and a mixed-type inhibition for *h*BChE for **1dA** ($p < 0.05$), which is consistent with the Lineweaver−Burk plot, used for visualization of obtained data (Figure 2). This finding confirms that all tested derivatives are reversible cholinesterase inhibitors.

For the derivative **1dC**, the intersection of lines is placed above the *x*-axis, indicating a mixed-mode of *h*AChE inhibition, meaning a reversible binding mode to both the free enzyme and enzyme−substrate complex, with higher affinity to the free enzyme ($K_i < K_i'$). K_m was increased, and V_{max} was reduced at a higher concentration of the inhibitor. **1dC** has an affinity to the free *h*AChE and enzyme−substrate complex.

In the case of *h*BChE, the intersection of lines is above the *x*-axis for **1dA**, which shows a mixed-type inhibition, meaning a

https://doi.org/10.1021/acschemneuro.1c00184
ACS Chem. Neurosci. 2021, 12, 1698−1715

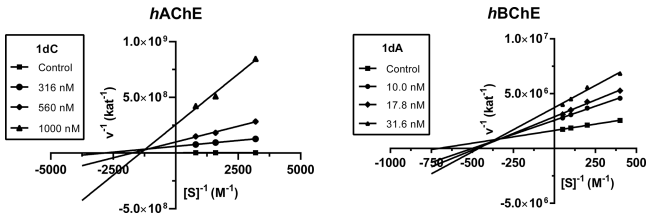

Figure 2. Steady-state inhibition of *h*AChE and *h*BChE substrate hydrolysis by compounds **1dC** and **1dA** at different concentrations. Lineweaver–Burk plots of initial velocity at increasing substrate concentrations (*h*AChE = 0.16–1.25 mM; *h*BChE = 2.5–20.0 mM) are presented. Lines were derived from a linear regression of the data points.

reversible binding mode to both the free enzyme and enzyme–substrate complex, with higher affinity to the free enzyme ($K_i < K_i'$). K_m was slightly increased, and V_{max} was reduced at a higher concentration of both inhibitors.

The K_i value of 6.7 ± 2.0 nM and K_i' value of 15.5 ± 2.7 nM were determined for **1dC** for *h*AChE. For **1dA**, the K_i value of 6.2 ± 1.6 nM and K_i' value 19.4 ± 2.6 nM were found for *h*BChE.

HepG2 Cytotoxicity, Antioxidant Activity, and *In Vitro* Estimation of the BBB Penetration. According to *h*AChE/*h*BChE inhibitory activities, 12 compounds were selected for further analysis. Attention was also paid to preserve structural diversity among the three tacrine subsets as well as the PHTs while accounting for the tether length. Cell viability was assessed on a liver hepatocellular carcinoma (HepG2) cell line using the MTT (3-(4,5-dimethylthiazol-2-yl)-2,5-diphenyl-tetraziolium bromide) reduction assay.[59] Measurement of compounds' cytotoxicity was carried out after 24 h incubation. All selected tacrine-PHTs exerted a rather higher cytotoxicity (IC_{50} values from 5.6 to 13.5 μM) compared to that of the reference tacrine and PHT (Table 2). This might be associated with increased molecular weight and lipophilicity. A similar trend has already been discussed recently, and it does not reflect or give any clear prospect for the *in vivo* toxicological profile.[49,60−62] Importantly, the most active hybrids exerted their activities in a low nanomolar range which is 3 orders of magnitude lower than calculated IC_{50} cytotoxicity values.

For a preliminary assessment of the antioxidant properties of the hybrids, we employed the operationally simple and widely used DPPH method.[63] No DPPH scavenging activity was found in this family; only PHT itself exerted weak antioxidant activity (Table S1). Loss of activity may be attributed to the *N*-alkylation of the PHT core, as this assay is based on the principle that the DPPH radical, by accepting a hydrogen atom from the scavenger molecule, is reduced to the DPPH-H form with a resulting decrease in absorbance. Thus, a secondary amine is necessary to preserve PHT antioxidant properties in this assay. This is in line with previously reported data pointing out that *N*-unsubstituted PHT derivatives were more efficient than those with amide groups.[30]

Furthermore, four selected hybrids (**1bC**, **1dC**, **2dA**, and **2dC**) were evaluated *in vitro* for their potential ability to cross the blood–brain barrier (BBB) using the cell monolayer based on a Madin-Darby Canine Kidney (MDCK) cell line as a model of BBB. On the basis of the achieved results, all tested compounds were predicted to enter the CNS (Table 2).

Table 2. Cytotoxicity of Tested Compounds in HepG2 Cells after 24 h and the MDCK Determination for Potential BBB Penetration

	HepG2 cell	BBB penetration estimation	
compound	IC_{50} (μM) ± SEM[b]	*Papp* ± SEM[b] ($\times 10^{-6}$ cm s^{-1})	CNS (+/−)
1aA	8.2 ± 0.7	n.t.[a]	n.t.
2aA	6.4 ± 0.3	n.t.	n.t.
3aC	6.9 ± 0.3	n.t.	n.t.
1bC	11.8 ± 0.7	18.9 ± 5.1	+
2bC	13.5 ± 1.7	n.t.	n.t.
1cB	5.0 ± 0.2	n.t.	n.t.
1dA	7.8 ± 0.1	n.t.	n.t.
1 dB	5.6 ± 0.5	n.t.	n.t.
1dC	13.1 ± 0.4	8.4 ± 3.7	+
2dA	5.6 ± 0.5	14.4 ± 7.2	+
2dC	6.0 ± 0.4	5.1 ± 1.7	+
3dC	8.2 ± 0.6	n.t.	n.t.
tacrine[c]	170.0 ± 3.6	25.0 ± 3.4	+
phenothiazine	>126	n.t.	n.t.
donepezil		20.7 ± 3.4	+
testosterone		17.4 ± 4.0	+
7-MEOTA[c]	44.0 ± 3.4	17.0 ± 3.6	+
sulfasalazine		0.1 ± 0.1	−
cefuroxime		0.1 ± 0.1	−
obidoxime		1.0 ± 0.2	−

[a]n.t. = not tested. [b]The results are expressed as the mean of a minimum of three experiments; BBB penetration measurements predict that the test compounds have the potential to passively pass the BBB. *Papp* values correspond to those of standard drugs with high CNS permeability. [c]Data taken from ref 64.

Inhibition of $\tau_{(306-336)}$ Peptide Aggregation. In the human brain, the τ protein exists in different isoforms which share a common third repeat domain (R3, residues 306–336). Mutagenesis studies have highlighted that the R3 domain plays a role in inducing τ aggregation,[65] and it is able to induce aggregation of the microtubule-binding region of τ in cells.[66] Based on these considerations, τ peptide 306–336 ($\tau_{(306-336)}$) is a suitable self-assembly model of the microtubule-binding domain in τ protein.[67] The *in vitro* aggregation of this τ fragment can be used to enable the preliminary prioritization of potential τ inhibitors.

Hybrids containing the 6-chloro-tacrine moiety were selected to be assayed, because the most potent *h*AChE inhibitor (**1dC**) belongs to this subseries. Analogues with a shorter linker chain were included in the study to assess the effect of the linker chain length on $\tau_{(306-336)}$ peptide aggregation. Finally, the analogue of derivative **2dC** bearing a chloro-substituent at the PHT moiety was also assayed being the second most potent *h*AChE inhibitor among the tacrine-PHT hybrids under investigation.

Inhibition experiments were performed by incubating $\tau_{(306-336)}$ peptide at 50 μM in the presence of selected hybrids (1:1 ratio). Formation of τ fibrils was monitored by using thioflavin T (ThT) as fluorescence probe.[14] Fluorescence intensity was scanned every 10 min for 16 h. Estimation of the inhibitory potency (%) was carried out by comparing fluorescence values at the plateau in the presence and in the absence of the inhibitor.

All selected hybrids significantly inhibited $\tau_{(306-336)}$ aggregation with differences falling in a narrow range (from

https://doi.org/10.1021/acschemneuro.1c00184
ACS Chem. Neurosci. 2021, 12, 1698−1715

50.5 to 62.1%) at 50 μM, while neither tacrine nor PHT were able to significantly interfere with $\tau_{(306-336)}$ aggregation (Figure 3). Based on the results, our conclusion is that the chain length

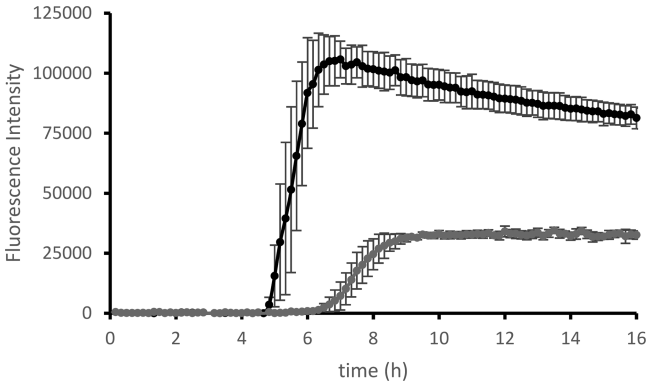

Figure 3. Averaged fluorescence profile of $\tau_{(306-336)}$ peptide aggregation in the absence (black line) and in the presence of **1cC** (gray line); $\tau_{(306-336)}$ and **1cC** were both at 50 μM, at 1:1 ratio. Fibril formation was monitored using ThT as fluorescent dye. λexc = 446 nm, λem = 490 nm. Results are based on three independent experiments.

influences the inhibitory potency, with optimal values being two or three methylene units. Introduction of a chlorine atom at the PHT moiety does not significantly affect the antiaggregating properties (compare activity of derivatives **1dC** and **2dC**) (Table 3).

Table 3. Antiaggregating Properties of Selected Tacrine-PHT Hybrids toward $\tau_{(306-336)}$ Self-Aggregation

compound	inhibition of τ(306−336) peptide self-aggregation (%) ± SEM[a]
1aC	55.6 ± 1.8
1bC	62.1 ± 5.4
1cC	61.1 ± 0.3
1dC	50.5 ± 1.7
2dC	51.9 ± 0.6
tacrine	∼5
phenothiazine	<5

[a]The results are the mean of at least two independent measurements each performed in triplicate. $\tau_{(306-336)}$ and tested compounds were both at 50 μM, at 1:1 ratio.

Of note, all selected derivatives were able not only to reduce the amount of fibril formed (lower the fluorescence value at the plateau) but also to significantly delay (by about 1.5−2 h) the exponential phase of the aggregation profile (see Figure 3, aggregation profiles in the absence and the presence of **1cC**, the most potent inhibitor among those assayed, as representative example) which can likely be attributed to a stabilization of the starting β-sheet conformer of the τ fragment.

Inhibition of Self-Induced Aβ_{1-42} Aggregation. Because the formation of Aβ oligomers and their accumulation into amyloid plaques is still considered as a triggering point in AD, there is a demand for the development of effective anti-Aβ drugs.[68] It is known that β-sheet-rich aromatic residues of Aβ play a pivotal role in the self-aggregation process; thus, aromatic-containing compounds should be able to intermolecularly recognize these regions and prevent aggregation via π-stacking interactions.[69−71] This phenomenon has already been confirmed in some MB and PHT derivatives.[34] Thus, compounds **1(a−d)C** and **2dC** were selected and were evaluated for their ability to inhibit self-induced Aβ_{1-42} aggregation (at an inhibitor/Aβ ratio of 1/1, 50 μM concentration, similar to $\tau_{(306-336)}$ peptide aggregation assay). Tacrine and PHT were selected as parent compounds, and MB and doxycycline were used as positive references. The aggregation of amyloidogenic isoform Aβ_{1-42} was inspected by a ThT-based fluorescence assay, which allows for the monitoring of amyloid fibril formation.[72]

According to the obtained results, the length of the linker proved to be crucial for anti-Aβ properties in a comparable manner to previous findings.[73,74] This accounts for five methylene tethered heterodimers (**1dC** and **2dC**) showing excellent inhibitory potency (% inhibition > 70%). Conversely and interestingly, short-chained derivatives (**1(a−c)C**) were not active (Table 4). Anti-Aβ property in **1dC** and **2dC** might

Table 4. Inhibition of Aβ_{1-42} Aggregation Produced by the Tested Compounds at 50μM Concentration (1/1 Ratio with Amyloid)

compound[a]	inhibition of Aβ_{1-42} aggregation ± SEM (%)[b]
1aC	n.a.[c]
1bC	n.a.[c]
1cC	n.a.[c]
1dC	74.1 ± 18.8
2dC	75.7 ± 0.1
tacrine	12.9 ± 12.9
methylene blue	∼100
phenothiazine	49.1 ± 15.7
doxycycline	99.0 ± 3.0

[a]Inhibition of Aβ_{1-42} aggregation was measured in the presence of compounds in the ratio Aβ_{1-42}/compound 1:1 at 50 μM. [b]The results are the mean of three independent measurements each performed in duplicate. [c]n.a. stands for not active; i.e., no significant inhibition was observed at compound concentration of 50 μM.

be attributed to (i) improved ligand flexibility and (ii) a longer spacer between two pharmacophores (five methylenes) that can allow for the contacting of two parallel β-strands of Aβ_{1-42};[75] however, further research is needed to prove this hypothesis. Both highlighted compounds (**1dC** and **2dC**) showed superior activity to tacrine and PHT, further justifying the tacrine-PHT combination. On the other hand, neither **1dC** nor **2dC** reached the efficacy of MB, which was able to completely inhibit Aβ aggregation at 50 μM, a datum that is consistent to other studies.[76]

Neurotoxicity in Primary Rat CGNs. The data collected so far made **1dC** and **2dC** an interesting starting point on multiple fronts by acting as cholinesterase/τ-aggregation/Aβ-aggregation inhibitors that cross the BBB. To further evaluate the potential of these PHT-tacrine hybrids, neurotoxicity against primary cultures of cerebellar granule neurons (CGNs) was tested. Following an experimental protocol we recently applied for analogous PHT derivatives,[31] compounds were tested at 5 μM concentration, and viability was assessed by using two different readouts, i.e., MTT and condensed (apoptotic) nuclei counting using Hoechst fluorescent dye. Intriguingly, whereas both compounds reduced viability over 50% in the MTT (5 μM; Figure 4), only a 33% reduction for **1dC** and a 15% reduction for **2dC** of cell death were observed

https://doi.org/10.1021/acschemneuro.1c00184
ACS Chem. Neurosci. 2021, 12, 1698−1715

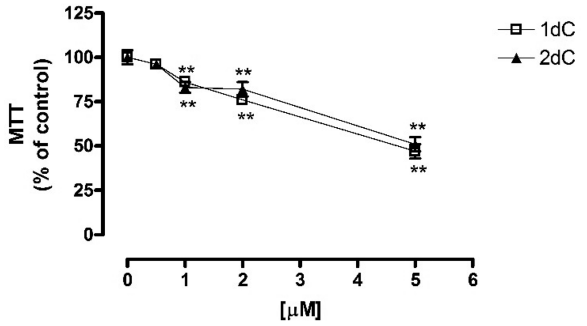

Figure 4. Neurotoxicity of **1dC** and **2dC** on primary rat CGNs after 24 h treatment. Results are expressed as percentage of controls and are the mean ± SE of three experiments, in quadruplicate. ** $p < 0.01$ compared to control conditions (0 μM) using one-way ANOVA and Bonferroni's posthoc test.

microphotographically after Hoechst staining (Figure 5). Importantly, the neurotoxicity profile revealed by fluorescent

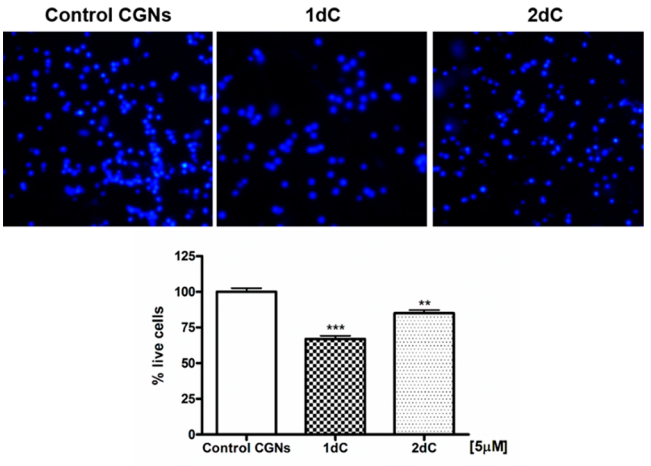

Figure 5. Live cell counting following Hoechst staining to test the toxicity of **1dC** and **2dC** compounds toward differentiated CGNs after 24 h treatment. Results are expressed as percentage of live cell counting following Hoechst staining. Results are the mean ± SE of five images. **$p < 0.01$ ***$p < 0.001$ compared to control CGNs, Student's t test.

staining of the condensed or fragmented nuclei assay mirrors that of chlorpromazine, a widely used CNS-directed drug.[31] The data obtained suggest that the MTT assay may produce false negative results when used to examine the viability of cells treated with PHT-based hybrids on this cell line.

Safety Evaluation and Verification of Brain Distribution *In Vivo*. Considering the relatively low neurotoxicity profile together with strong anticholinesterase activity, good τ antiaggregating properties, and predicted capability to cross the BBB, we continued with **1dC** *in vivo* testing. The reason to perform such an evaluation with **1dC** would be to provide a more clear outlook, specifically because (i) the mechanism underlying the hepatotoxicity of tacrine has not yet been fully elucidated and because (ii) the toxicity mechanism of tacrine might not be translated to the synthesized hybrids, which impose a novel chemotype. Preliminary safety and brain distribution studies were performed on Balb/c mice. Notably, no clinical sign of toxicity was observed in control mice as well as in **1dC**-treated mice. Necropsy revealed no macroscopic pathology of internal organs of the chest and abdominal cavity. Blood biochemistry (Table 5) as well as histopathological examination of intestine and mesentery, liver, and kidneys did not show any abnormalities. Positively, while tacrine has been reported to induce elevation in serum alanine aminotransferase (ALT) activity, which is indicative of hepatic injury in 30−50% of the patients,[62] this biomarker was not altered upon **1dC** administration. Thus, the administered dose of 14 mg/kg (i.p.) can be considered safe for further *in vivo* experiments.

The maximal concentration of hybrid **1dC** in plasma was achieved 30 min after i.p. administration; in subsequent time intervals, a gradual decrease was observed. The maximal brain concentration was also reached after 30 min (6.6 nM) and was relatively stable for all time intervals (Table 6) up to 120 min.

Table 6. *In Vivo* BBB Permeability Estimation of 1dC in Mice[a]

	blood	brain	ratio
time (min)	nM	nM	%
30	417 ± 46	6.6 ± 1.7	1.6
60	274 ± 56	3.7 ± 0.4	1.3
120	205 ± 21	4.9 ± 0.6	2.4

[a]Results are expressed as mean ± SEM, $n = 4$.

In light of these data and those related to the inhibitory activity against *h*AChE (IC_{50} 8.0 ± 0.4 nM) and the selectivity index (Table 1), hybrid **1dC** should be able to inhibit AChE at the central level. The relatively low elimination from the brain tissue suggests a potential for accumulation after repeated administration as in the case of tacrine.[77]

CONCLUSIONS

In summary, 36 novel hybrids were prepared by a facile three-step synthesis. Screening for cholinesterase inhibitory activity revealed that all the compounds were efficient inhibitors of cholinesterase enzymes with activities ranging from the micromolar to one-digit nanomolar scales. Activity and selectivity depended on the type of tacrine fragment (either unsubstituted, chloro-derivative, or methoxy-derivative) and the length of the linker used to connect the two pharmacophore units, highlighting the two-methylene linker for *h*BChE-selective compounds and the five-methylene linker for *h*AChE-selective compounds. No clear SAR for substituents at the PHT fragment could be drawn, thus considering that these do not play a key role in the modulation of the inhibitory potency toward either cholinesterase. Of note, 7-MEOTA and 2-trifluoromethyl-PHT derivatives always

Table 5. Selected Biochemical Parameters Assessed in Blood Plasma 24 h after Administration of Hybrid 1dC[a]

	glucose (mg/dL)	urea (mg/dL)	creatinine (μg/dL)	ALT (U/L)	AST (U/L)	ALP (U/L)	amylase (U/L)
control	161 ± 17	44 ± 6	45 ± 6	24 ± 1	63 ± 7	84 ± 8	2459 ± 97
1dC	193 ± 15	44 ± 5	55 ± 8	21 ± 1	57 ± 6	82 ± 9	2380 ± 182

[a]Results are expressed as mean ± SEM, $n = 6$ (3 males and 3 females).

https://doi.org/10.1021/acschemneuro.1c00184
ACS Chem. Neurosci. 2021, 12, 1698−1715

resulted in a poor-to-moderate inhibitory activity. The hybrids bearing an unsubstituted PHT and tacrine or 6-chlorotacrine moieties showed the highest AChE/BChE activity. Specifically, **1dC** was the most effective and selective *h*AChE inhibitor with IC_{50} = 8 nM, while **1aA** was the most potent and selective *h*BChE inhibitor with IC_{50} = 15 nM. Of note, inhibitory activity toward AChE by **1dC** is comparable to that of the drug donepezil. Importantly, 6-chlorotacrine hybrids **1(a−d)C** and **2dC** not only inhibited $\tau_{(306-336)}$ peptide aggregation but also significantly delayed the exponential phase of aggregation. Furthermore, the remarkable ability to inhibit self-induced $A\beta_{1-42}$ aggregation was found for compounds **1dC** and **2dC**. Notwithstanding the new hybrid's affected cell viability when tested on HepG2 cells and cerebellar granule neurons (MTT readout), no pathophysiological abnormality was observed after i.p. administration of **1dC** to mice at 14 mg/kg. Hence, *in vivo* experiments showed that **1dC** was relatively safe, and it was able to permeate the BBB and inhibit the brain AChE. Further *in vivo* experiments to fully understand the therapeutic potential of **1dC** as a multitarget-directed ligand for AD are warranted.

METHODS

Chemistry. *General Synthetic Methods.* The column chromatography was performed using silica gel 100 and Sigma-Aldrich silica gel grade 9385, 60 Å, 230−400 mesh at atmospheric pressure. The analytical thin-layer chromatography (TLC) was carried out using 0.20 mm silica gel 60 F254 plates (Merck, Germany), which were visualized by exposure to ultraviolet light (254 nm) and phosphomolybdic acid (PMA) and bromocresol green (BCG) stains. The NMR spectra were recorded on a Varian S500 spectrometer (500 and 126 MHz) and on a Varian VXR 400 (400 MHz for ^{1}H and 100 MHz for ^{13}C). Chemical shifts are reported in δ parts per million (ppm) referenced to an internal $SiMe_4$ standard for ^{1}H NMR and $CDCl_3$-*d* ($CHCl_3$-*dl*; 7.26 (D); 77.16 (C) ppm), CD_3OD (CH_3OH-*dl*; 3.35, 4.78 (D), 49.3 (C) ppm), or hexadeuteriodimethyl sulfoxide (DMSO-*d6*; 2.50 (D), 39.7 (C) ppm). Chemicals were purchased from Sigma-Aldrich Co. LLC and were used without additional purification. CEM Explorer SP 12 S Class was used for microwave irradiation. The final compounds were analyzed by LC-MS consisting of UHLPC Dionex Ultimate 3000 RS coupled with a Q Exactive Plus orbitrap mass spectrometer (Thermo Fisher Scientific, Bremen, Germany) to obtain high resolution mass spectra. Gradient LC analysis confirmed >95% purity.

*5-(1,3-Dioxo-2,3-dihydro-1H-isoindol-2-yl)pentanal (**9**).* (**A**) 5-Amino-1-pentanol (**8**; 33.93 mmol) and phthalic anhydride (33.93 mmol) were added into the oven-dried round-bottom flask. The mixture was stirred at 145 °C under Ar atmosphere for 30 min. The resulting residue, with no need of further purification, was dried on vacuum pump affording 5-(1,3-dioxo-2,3-dihydro-1*H*-isoindol-2-yl)-pentanol as a light yellow oil with quantitative yield. ^{1}H NMR (500 MHz, $CDCl_3$-*d*): δ 7.86−7.81 (m, 2H), 7.73−7.69 (m, 2H), 3.70 (t, *J* = 7.2 Hz, 2H), 3.64 (t, *J* = 6.5 Hz, 2H), 1.78−1.67 (m, 2H), 1.67−1.57 (m, 2H), 1.48−1.38 (m, 2H). ^{13}C NMR (126 MHz, $CDCl_3$): δ 168.45, 133.85, 132.08, 123.14, 62.57, 37.81, 32.14, 28.31, 22.99. (**B**) $(COCl)_2$ (40.72 mmol) was added to anhydrous DCM (60 mL) containing DMSO (74.65 mmol) at −45 °C under Ar atmosphere. After the mixture was stirred for 5 min, 5-(1,3-dioxo-2,3-dihydro-1*H*-isoindol-2-yl)pentanol (33.93 mmol) dissolved in anhydrous DCM was added dropwise. After the mixture was stirred for another 15 min, diisopropylethylamine (DIPEA; 101.79 mmol) was added portion-wise. The reaction was cooled to −30 °C and stirred for an additional 30 min. Finally, the solvent was removed, and the residue was diluted with EA allowing for the formation of a white precipitate which was removed by filtration. The filtrate was washed once with 150 mL of 6% $NaHCO_3$ and three times with 150 mL of H_2O. The organic layer was dried with anhydrous Na_2SO_4 and concentrated affording **9** as a light red oil. Yield = 77% after two steps. ^{1}H NMR (500 MHz, $CDCl_3$-*d*): δ 9.73 (s, 1H), 7.84−7.77 (m, 2H), 7.73−7.66 (m, 2H), 3.68 (t, *J* = 6.8 Hz, 2H), 2.51−2.45 (m, 2H), 1.76−1.60 (m, 4H). ^{13}C NMR (126 MHz, $CDCl_3$): δ 201.80, 168.32, 133.93, 132.01, 123.18, 43.15, 37.39, 27.93, 19.19.

*2-(5,5-Diethoxypentyl)-2,3-dihydro-1H-isoindole-1,3-dione (**10**).* Compound **9** (5.01 mmol) and *p*-toluenesulfonic acid monohydrate (0.05 mmol) were dissolved in absolute EtOH under Ar atmosphere. The solution was further bubbled with Ar. Then, triethyl orthoformate (5.01 mmol) was slowly added, and the mixture was stirred and bubbled with Ar for 3 h at RT. EtOH was evaporated, and the residue was diluted with DCM (70 mL) and saturated with $NaHCO_3$ (100 mL). The mixture was extracted three times with DCM (3 × 70 mL), and the organic layers were collected, dried with anhydrous Na_2SO_4, and filtered off. The filtrate was concentrated under reduced pressure and purified by column chromatography (PE/EA = 5:1) affording **10** as a colorless oil. Yield = 74%. ^{1}H NMR (500 MHz, $CDCl_3$-*d*): δ 7.86−7.81 (m, 2H), 7.73−7.68 (m, 2H), 4.47 (t, *J* = 5.7 Hz, 1H), 3.69 (t, *J* = 7.3 Hz, 2H), 3.66−3.59 (m, 2H), 3.52−3.44 (m, 2H), 1.76−1.62 (m, 4H), 1.46−1.38 (m, 2H), 1.23−1.14 (m, 6H). ^{13}C NMR (126 MHz, $CDCl_3$): δ 168.35, 133.80, 132.14, 123.11, 102.66, 61.03, 37.88, 33.14, 28.38, 22.06, 15.29.

*Preparation of Phenothiazine Intermediates **16**−**27**.* In the dried round-bottom flask, **6**, **7**, **10**, or **12** (2.4 mmol) and **13**, **14**, or **15** (2 mmol) were dissolved in dry DCM (20 mL) under nitrogen atmosphere. Trifluoroacetic acid (TFA; 26 mmol) and triethylsilane (TES; 5 mmol) was then added dropwise, and the reaction mixture was stirred for 2 h at room temperature. Then, the reaction mixture was cooled to 0 °C and slowly neutralized with addition of saturated $NaHCO_3$ (until pH = 7−8). The mixture was extracted with DCM 3 × 20 mL. The organic layers were collected, dried with anhydrous Na_2SO_4, and filtered. The filtrate was concentrated under reduced pressure and purified by column chromatography affording **16**−**27**.

*N-[2-(10H-Phenothiazin-10-yl)ethyl]-2,2,2-trifluoroacetamide (**16**).* The resulting residue was purified by column chromatography (PE/EA = 9:1) affording **16** as a dark yellow viscous oil. Yield = 41%. ^{1}H NMR (400 MHz, $CDCl_3$-*d*): δ 7.23−7.16 (m, 4H), 7.03−6.89 (m, 4H), 6.80 (bs, 1H), 4.14 (t, *J* = 5.9 Hz, 2H), 3.71 (q, *J* = 5.9 Hz, 2H). ^{13}C NMR (100 MHz, $CDCl_3$): δ 144.55, 127.90, 127.61, 126.80, 123.49, 116.16, 46.05, 36.82.

*N-[2-(2-Chloro-10H-phenothiazin-10-yl)ethyl]-2,2,2-trifluoroacetamide (**17**).* The resulting residue was purified by column chromatography (PE/EA = 9:1) affording **17** as a purple viscous oil. Quantitative yield. ^{1}H NMR (400 MHz, $CDCl_3$-*d*): δ 7.28−7.15 (m, 2H), 7.15−7.07 (m, 1H), 7.07−6.85 (m, 3H), 6.83−6.68 (m, 1H), 4.11 (t, *J* = 5.9 Hz, 2H), 3.71 (q, *J* = 5.9 Hz, 2H). ^{13}C NMR (100 MHz, $CDCl_3$): δ 145.94, 143.78, 133.65, 128.38, 127.99, 127.82, 126.39, 125.14, 123.91, 123.40, 116.53, 116.37, 46.13, 36.75.

*N-{2-[2-(Trifluoromethyl)-10H-phenothiazin-10-yl]ethyl}-2,2,2-trifluoroacetamide (**18**).* The resulting residue was purified by column chromatography (PE/EA = 9:1) affording **18** as a dark yellow viscous oil. Quantitative yield. ^{1}H NMR (400 MHz, $CDCl_3$-*d*): δ 7.36−7.14 (m, 4H), 7.14−6.91 (m, 2H), 6.73−6.59 (m, 1H), 4.17 (t, *J* = 5.9 Hz, 2H), 3.73 (q, *J* = 5.9 Hz, 2H).

*N-[3-(10H-Phenothiazin-10-yl)propyl]acetamide (**22**).* The resulting residue was purified by column chromatography (EA/DCM = 1:1) affording **22** as a white-brown solid. Yield = 99%. ^{1}H NMR (400 MHz, $CDCl_3$-*d*): δ 7.24−7.13 (m, 4H), 7.01−6.86 (m, 4H), 6.16 (bs, 1H), 3.96 (t, *J* = 6.0 Hz, 2H), 3.33 (q, *J* = 6.0 Hz, 2H), 1.99 (p, *J* = 6.1 Hz, 2H), 1.75 (s, 3H). ^{13}C NMR (100 MHz, $CDCl_3$): δ 170.16, 145.34, 127.75, 127.55, 125.64, 122.95, 115.87, 45.92, 38.53, 26.05, 22.97.

*N-[3-(2-Chloro-10H-phenothiazin-10-yl)propyl]acetamide (**23**).* The resulting residue was purified by column chromatography (PE/EA = 1:1) affording **23** as a white sticky foam. Yield = 94%. ^{1}H NMR (400 MHz, chloroform-*d*): δ 7.24−7.16 (m, 2H), 7.13−7.06 (m, 1H), 7.04−6.80 (m, 4H), 6.04 (s, 1H), 3.94 (t, *J* = 6.1 Hz, 2H), 3.35 (q, *J* = 6.1 Hz, 2H), 2.02 (q, *J* = 6.2 Hz, 2H), 1.83−1.78 (m, 3H).

*N-{3-[2-(Trifluoromethyl)-10H-phenothiazin-10-yl]propyl}-acetamide (**24**).* The resulting residue was purified by column

https://doi.org/10.1021/acschemneuro.1c00184
ACS Chem. Neurosci. 2021, 12, 1698−1715

chromatography (EA/DCM = 1:1) affording **24** as a yellow viscous oil. Yield = 83%. ^{1}H NMR (400 MHz, $CDCl_3$-*d*): δ 7.28−7.13 (m, 4H), 7.08−7.02 (m, 1H), 7.02−6.94 (m, 1H), 6.93−6.87 (m, 1H), 5.94 (bs, 1H), 3.97 (t, *J* = 6.2 Hz, 3H), 3.34 (q, *J* = 6.3 Hz, 2H), 2.06−1.95 (m, 2H), 1.80 (s, 3H). ^{13}C NMR (100 MHz, $CDCl_3$): δ 170.15, 145.80, 144.31, 127.92, 127.83, 127.78, 124.53, 123.54, 119.53, 119.49, 116.18, 112.17, 112.13, 45.74, 38.06, 26.20, 23.02.

*N-[4-(10H-Phenothiazin-10-yl)butyl]-2,2,2-trifluoroacetamide (**19**).* The resulting residue was purified by column chromatography (PE/EA = 7:1) affording **19** as a dark yellow viscous oil. Quantitative yield. ^{1}H NMR (400 MHz, $CDCl_3$-*d*): δ 7.20−7.12 (m, 4H), 6.98−6.89 (m, 2H), 6.89−6.81 (m, 2H), 6.31 (bs, 1H), 3.92 (t, *J* = 6.3 Hz, 2H), 3.33 (q, *J* = 6.7 Hz, 2H), 1.91−1.77 (m, 2H), 1.74−1.64 (m, 2H). ^{13}C NMR (100 MHz, $CDCl_3$): δ 145.09, 127.68, 127.33, 125.57, 122.76, 115.64, 46.36, 39.42, 26.37, 23.54.

*N-[4-(2-Chloro-10H-phenothiazin-10-yl)butyl]-2,2,2-trifluoroacetamide (**20**).* The resulting residue was purified by column chromatography (PE/EA = 9:1) affording **20** as a dark yellow viscous oil. Yield = 84%. ^{1}H NMR (400 MHz, $CDCl_3$-*d*): δ 7.20−7.13 (m, 2H), 7.07−7.03 (m, 1H), 6.99−6.92 (m, 1H), 6.92−6.88 (m, 1H), 6.87−6.83 (m, 1H), 6.83−6.80 (m, 1H), 3.88 (t, *J* = 6.3 Hz, 2H), 3.34 (q, *J* = 6.7 Hz, 2H), 1.87−1.77 (m, 2H), 1.75−1.66 (m, 2H). ^{13}C NMR (100 MHz, $CDCl_3$): δ 146.45, 144.31, 133.37, 128.13, 127.75, 127.51, 125.31, 124.06, 123.21, 122.59, 115.98, 115.94, 46.53, 39.38, 26.34, 23.56.

*N-{4-[2-(Trifluoromethyl)-10H-phenothiazin-10-yl]butyl}-2,2,2-trifluoroacetamide (**21**).* The resulting residue was purified by column chromatography (PE/EA = 7:1) affording **21** as a yellow viscous oil. Yield = 85%. ^{1}H NMR (400 MHz, $CDCl_3$-*d*): δ 7.28−7.11 (m, 4H), 7.05−6.93 (m, 2H), 6.92−6.84 (m, 1H), 6.29 (bs, 1H), 3.94 (t, *J* = 6.3 Hz, 2H), 3.34 (q, *J* = 6.6 Hz, 2H), 1.87−1.76 (m, 2H), 1.77−1.65 (m, 2H). ^{13}C NMR (100 MHz, $CDCl_3$): δ 156.66, 145.63, 144.14, 127.79, 127.74, 127.71, 124.59, 123.41, 119.38, 119.34, 116.01, 111.98, 46.61, 39.38, 26.32, 23.57.

*2-[5-(10H-Phenothiazin-10-yl)pentyl]-2,3-dihydro-1H-isoindole-1,3-dione (**25**).* The resulting residue was purified by column chromatography (PE/EA = 5:1) affording **25** as a dark yellow viscous oil. Quantitative yield. ^{1}H NMR (500 MHz, $CDCl_3$-*d*): δ 7.87−7.80 (m, 2H), 7.75−7.68 (m, 2H), 7.17−7.11 (m, 2H), 7.11−7.07 (m, 2H), 6.95−6.81 (m, 3H), 3.90−3.79 (m, 2H), 3.71−3.66 (m, 2H), 1.91−1.81 (m, 2H), 1.76−1.67 (m, 2H), 1.54−1.44 (m, 2H). ^{13}C NMR (126 MHz, $CDCl_3$): δ 168.36, 133.80, 132.10, 127.39, 127.15, 123.14, 123.10, 122.36, 115.40, 70.28, 47.00, 37.73, 28.13, 24.04.

*2-[5-(2-Chloro-10H-phenothiazin-10-yl)pentyl]-2,3-dihydro-1H-isoindole-1,3-dione (**26**).* The resulting residue was purified by column chromatography (PE/EA = 5:1) affording **26** as a dark purple viscous oil. Yield = 89%. ^{1}H NMR (500 MHz, $CDCl_3$-*d*): δ 7.87−7.81 (m, 2H), 7.74−7.68 (m, 2H), 7.18−7.12 (m, 1H), 7.11−7.06 (m, 1H), 7.00−6.96 (m, 1H), 6.95−6.89 (m, 1H), 6.89−6.82 (m, 2H), 6.83−6.78 (m, 1H), 3.82 (t, *J* = 7.0 Hz, 2H), 3.68 (t, *J* = 7.1 Hz, 2H), 1.89−1.80 (m, 2H), 1.76−1.66 (m, 2H), 1.53−1.44 (m, 2H). ^{13}C NMR (126 MHz, $CDCl_3$): δ 168.36, 146.49, 144.41, 133.82, 133.80, 132.10, 127.85, 127.47, 127.35, 123.16, 123.11, 122.83, 122.19, 115.74, 115.71, 47.09, 37.68, 28.10, 26.23, 23.95.

*2-{5-[2-(Trifluoromethyl)-10H-phenothiazin-10-yl]pentyl}-2,3-dihydro-1H-isoindole-1,3-dione (**27**).* The resulting residue was purified by column chromatography (PE/EA = 5:1) affording **27** as a dark yellow viscous oil. Quantitative yield. ^{1}H NMR (500 MHz, $CDCl_3$-*d*): δ 7.87−7.80 (m, 2H), 7.76−7.68 (m, 2H), 7.21−7.10 (m, 3H), 7.10−7.07 (m, 1H), 7.02−6.99 (m, 1H), 6.97−6.90 (m, 1H), 6.90−6.84 (m, 1H), 3.88 (t, *J* = 7.0 Hz, 2H), 3.70−3.65 (m, 2H), 1.90−1.79 (m, 2H), 1.79−1.66 (m, 2H), 1.53−1.46 (m, 2H).

*General Procedure for the Hydrolysis of Trifluoroacetamides **16**−**21** to Primary Amines **28**−**33**.* Compounds **16**−**21** (1.5 mmol) and K_2CO_3 (12 mmol) were dissolved in the mixture of MeOH/H_2O 2:1 (12 + 6 mL). The mixture was stirred overnight at room temperature. The solvents were evaporated, and the precipitate was diluted with H_2O (20 mL) and extracted with DCM (3× 20 mL). The organic layers were collected, dried with anhydrous Na_2SO_4, and filtered. The filtrate was concentrated under reduced pressure to afford **28**−**33** without any need for further purification.

*2-(10H-Phenothiazin-10-yl)ethan-1-amine (**28**).* This compound is a dark yellow viscous oil with yield = 88%. ^{1}H NMR (400 MHz, $CDCl_3$-*d*): δ 7.22−7.08 (m, 4H), 7.03−6.83 (m, 4H), 3.99 (t, *J* = 5.9 Hz, 2H), 3.06 (t, *J* = 5.9 Hz, 2H), 1.45 (bs, 2H). ^{13}C NMR (100 MHz, $CDCl_3$): δ 145.22, 127.59, 127.23, 125.88, 122.69, 115.77, 50.52, 38.85.

*2-(2-Chloro-10H-phenothiazin-10-yl)ethan-1-amine (**29**).* This compound is a dark purple viscous oil with quantitative yield %. ^{1}H NMR (400 MHz, $CDCl_3$-*d*): δ 7.23−7.10 (m, 2H), 7.10−7.03 (m, 1H), 7.01−6.80 (m, 4H), 3.96 (t, *J* = 5.9 Hz, 2H), 3.06 (t, *J* = 5.9 Hz, 2H), 1.29 (bs, 2H).

*2-[2-(Trifluoromethyl)-10H-phenothiazin-10-yl]ethan-1-amine (**30**).* This compound is a dark yellow viscous oil with quantitative yield %. ^{1}H NMR (400 MHz, $CDCl_3$-*d*): δ 7.25−7.12 (m, 4H), 7.08−7.04 (m, 1H), 7.00−6.93 (m, 1H), 6.93−6.88 (m, 1H), 4.00 (t, *J* = 5.9 Hz, 2H), 3.06 (t, *J* = 5.9 Hz, 2H), 1.34 (bs, 2H).

*4-(10H-Phenothiazin-10-yl)butan-1-amine (**31**).* This compound is a dark brown viscous oil with yield = 82%. ^{1}H NMR (400 MHz, $CDCl_3$-*d*): δ 7.16−7.09 (m, 4H), 6.92−6.87 (m, 2H), 6.87−6.82 (m, 2H), 3.86 (t, *J* = 7.0 Hz, 2H), 2.68 (t, *J* = 7.0 Hz, 2H), 1.89−1.77 (m, 2H), 1.55 (p, *J* = 7.2 Hz, 2H), 1.29−1.17 (bs, 2H). ^{13}C NMR (100 MHz, $CDCl_3$): δ 145.23, 127.45, 127.15, 125.11, 122.38, 115.41, 47.10, 41.85, 31.12, 24.32.

*4-(2-Chloro-10H-phenothiazin-10-yl)butan-1-amine (**32**).* This compound is a dark brown viscous oil with yield = 93%. ^{1}H NMR (400 MHz, $CDCl_3$-*d*): δ 7.20−7.06 (m, 2H), 7.06−6.96 (m, 1H), 6.97−6.77 (m, 4H), 3.82 (t, *J* = 7.0 Hz, 2H), 2.69 (t, *J* = 7.0 Hz, 2H), 1.88−1.73 (m, 2H), 1.62−1.44 (m, 2H), 1.11 (bs, 2H). ^{13}C NMR (100 MHz, $CDCl_3$): δ 146.53, 144.50, 133.16, 127.89, 127.52, 127.35, 124.87, 123.60, 122.85, 122.20, 115.75, 115.73, 47.23, 41.79, 31.00, 24.19.

*4-[2-(Trifluoromethyl)-10H-phenothiazin-10-yl]butan-1-amine (**33**).* This compound is a dark yellow viscous oil with yield = 90%. ^{1}H NMR (400 MHz, $CDCl_3$-*d*): δ 7.20−7.15 (m, 2H), 7.15−7.09 (m, 2H), 7.03−6.99 (m, 1H), 6.97−6.90 (m, 1H), 6.89−6.84 (m, 1H), 3.88 (t, *J* = 7.0 Hz, 2H), 2.69 (t, *J* = 7.0 Hz, 2H), 1.90−1.74 (m, 2H), 1.62−1.50 (m, 2H), 1.21−1.14 (bs, 2H). ^{13}C NMR (100 MHz, $CDCl_3$): δ 145.68, 144.35, 130.02, 129.70, 127.59, 127.57, 127.46, 124.15, 123.06, 119.03, 119.00, 115.81, 111.84, 111.80, 47.27, 41.76, 30.94, 24.13.

*General Procedure for the Hydrolysis of Acetamides **22**−**24** to Primary Amines **34**−**36**.* Compounds **22**−**24** (1.5 mmol) and KOH (11.25 mmol) were dissolved in the mixture of MeOH/H_2O 2:1 (6 + 3 mL) in the microwave-sealed tube. The mixture was subjected to microwave irradiation (150 W) at 160 °C for 2 h. The reaction mixture was concentrated under reduced pressure and purified via column chromatography affording products **34**−**36**.

*3-(10H-Phenothiazin-10-yl)propan-1-amine (**34**).* The resulting residue was purified by column chromatography (DCM/MeOH/NH_3 (33% aq sol) = 15:1:01) affording **34** as a yellow viscous oil. Yield = 91%. Without characterization used directly into the next reactions.

*3-(2-Chloro-10H-phenothiazin-10-yl)propan-1-amine (**35**).* The resulting residue was purified by column chromatography (DCM/MeOH/NH_3 (33% aq sol) = 14:1:01) affording **35** as a yellow viscous oil. Yield = 65%. ^{1}H NMR (400 MHz, $CDCl_3$-*d*): δ 7.18−7.07 (m, 2H), 7.03−6.96 (m, 1H), 6.96−6.82 (m, 4H), 3.93 (t, *J* = 6.6 Hz, 2H), 3.32 (t, *J* = 6.7 Hz, 2H), 2.11 (p, *J* = 6.6 Hz, 2H). ^{13}C NMR (100 MHz, $CDCl_3$): δ 168.14, 146.47, 144.53, 133.20, 127.75, 127.38, 124.66, 123.38, 122.77, 122.13, 115.97, 115.89, 48.09, 44.86, 29.20, 27.71.

*3-[2-(Trifluoromethyl)-10H-phenothiazin-10-yl]propan-1-amine (**36**).* The resulting residue was purified by column chromatography (DCM/MeOH/NH_3 (33% aq sol) = 14:1:01) affording **36** as a yellow viscous oil. Yield = 85%. ^{1}H NMR (400 MHz, $CDCl_3$-*d*): δ 7.20−7.01 (m, 4H), 6.99−6.84 (m, 3H), 3.97 (t, *J* = 6.6 Hz, 2H), 3.31 (t, *J* = 6.6 Hz, 2H), 2.10 (p, *J* = 6.6 Hz, 2H). ^{13}C NMR (100 MHz, $CDCl_3$): δ 145.67, 144.34, 129.77, 127.61, 127.43, 127.32,

https://doi.org/10.1021/acschemneuro.1c00184
ACS Chem. Neurosci. 2021, 12, 1698−1715

123.92, 122.99, 118.94, 115.98, 112.05, 112.01, 48.00, 44.86, 29.11, 27.63.

*General Procedure for the Hydrolysis of Phthalimides **25**–**27** to Primary Amines **37**–**39**.* Compounds **25**–**27** (2.0 mmol) were dried in a round-bottom flask and dissolved in absolute EtOH under Ar atmosphere. Hydrazine hydrate (50–60% solution in H_2O; 1.0 mL) was slowly added, and the mixture was heated to reflux (90 °C) and kept stirred under Ar overnight (16 h). The next day, the white precipitate was filtered and washed with EtOH. The filtrate was concentrated under reduced pressure and purified by column chromatography affording products **37** – **39**.

*5-(10H-Phenothiazin-10-yl)pentan-1-amine (**37**).* The resulting residue was purified by column chromatography (DCM/MeOH/NH_3 (25% aq sol) = 9:1:0.1) affording **37** as a light yellow viscous oil. Yield = 82%. ^{1}H NMR (500 MHz, $CDCl_3$-*d*): δ 7.18–7.11 (m, 4H), 6.94–6.89 (m, 2H), 6.89–6.83 (m, 2H), 3.91–3.81 (m, 2H), 2.73–2.63 (m, 2H), 2.07 (bs, 2H), 1.87–1.76 (m, 2H), 1.51–1.41 (m, 4H). ^{13}C NMR (126 MHz, $CDCl_3$): δ 145.23, 127.41, 127.13, 125.04, 122.34, 115.40, 47.08, 41.73, 32.67, 26.61, 24.08.

*5-(2-Chloro-10H-phenothiazin-10-yl)pentan-1-amine (**38**).* The resulting residue was purified by column chromatography (DCM/MeOH/NH_3 (25% aq sol) = 9:1:0.1) affording **38** as a light yellow viscous oil. Yield = 74%. ^{1}H NMR (500 MHz, $CDCl_3$-*d*): δ 7.19–7.11 (m, 2H), 7.04–7.00 (m, 1H), 6.96–6.91 (m, 1H), 6.91–6.87 (m, 1H), 6.87–6.83 (m, 1H), 6.84–6.79 (m, 1H), 3.83 (t, *J* = 7.0 Hz, 2H), 2.69 (t, *J* = 6.5 Hz, 2H), 2.11 (bs, 2H), 1.85–1.76 (m, 2H), 1.54–1.41 (m, 4H). ^{13}C NMR (126 MHz, $CDCl_3$): δ 146.54, 144.50, 133.15, 127.88, 127.50, 127.35, 124.82, 123.57, 122.84, 122.18, 115.74, 47.22, 41.69, 32.51, 26.49, 24.03.

*5-[2-(Trifluoromethyl)-10H-phenothiazin-10-yl]pentan-1-amine (**39**).* The resulting residue was purified by column chromatography (DCM/MeOH/NH_3 (25% aq. sol.) = 9:1:0.1) affording **39** as a light yellow viscous oil. Yield = 75%. ^{1}H NMR (500 MHz, $CDCl_3$-*d*): δ 7.22–7.10 (m, 4H), 7.04–7.00 (m, 1H), 6.98–6.93 (m, 1H), 6.90–6.85 (m, 1H), 3.88 (t, *J* = 7.0 Hz, 2H), 2.74–2.64 (m, 2H), 1.87–1.84 (m, 2H), 1.84–1.76 (m, 2H), 1.54–1.41 (m, 4H). ^{13}C NMR (126 MHz, $CDCl_3$): δ 145.72, 144.41, 130.02, 129.69, 129.43, 127.60, 127.58, 127.48, 125.24, 124.13, 123.07, 119.06, 119.03, 119.00, 118.97, 115.84, 111.88, 111.85, 111.82, 111.79, 47.33, 41.83, 32.84, 26.51, 24.08.

General Procedure for the Coupling of N-Alkylated Phenothiazine with 9-Chloro-1,2,3,4-tetrahydroacridine Derivatives. Compounds **28**–**39** (0.20 mmol) and 9-chloro-1,2,3,4-tetrahydroacridines **A**–**C** (0.22 mmol) were melted and dissolved in phenol (0.3 mL) by heating gun at 90 °C in the microwave-sealed tube. The mixture was then subjected to microwave irradiation (150 W) at 180 °C for 90 min. The reaction mixture was diluted with 20 mL of DCM and a 20% solution of KOH (20 mL), following extraction with additional DCM (3 × 20 mL). The organic layers were collected, dried with anhydrous Na_2SO_4, and filtered. The filtrate was concentrated under reduced pressure and purified by column chromatography affording products **1**–**3(a**–**d)A**–**C**.

*N-[2-(10H-Phenothiazin-10-yl)ethyl]-1,2,3,4-tetrahydroacridin-9-amine (**1aA**).* The resulting residue was purified by column chromatography (PE/DCM/Tol/EtOH/NH_3 (33% aq sol) = 15:6:3:1:0.1) affording **1aA** as a yellow viscous oil. Yield = 52%. ^{1}H NMR (400 MHz, $CDCl_3$-*d*): δ 8.08–7.81 (m, 2H), 7.60–7.44 (m, 1H), 7.32–7.20 (m, 3H), 7.20–7.10 (m, 2H), 7.05–6.92 (m, 2H), 6.91–6.81 (m, 2H), 4.76 (bs, 1H), 4.05 (t, *J* = 5.2 Hz, 2H), 3.86 (t, *J* = 4.9 Hz, 2H), 2.99 (t, *J* = 6.5 Hz, 2H), 2.50 (t, *J* = 6.4 Hz, 2H), 1.81–1.67 (m, 2H), 1.69–1.54 (m, 2H). ^{13}C NMR (100 MHz, $CDCl_3$): δ 144.76, 128.70, 127.81, 127.46, 126.74, 123.95, 123.31, 122.89, 115.85, 47.19, 45.05, 33.23, 24.09, 22.59, 22.41. HRMS (ESI$^+$): $[M]^+$ = calculated for $C_{27}H_{26}N_3S^+$ (*m*/*z*), 424.184 19; found, 424.184 23. LC-MS purity > 95%.

*7-Methoxy-N-[2-(10H-phenothiazin-10-yl)ethyl]-1,2,3,4-tetrahydroacridin-9-amine (**1aB**).* The resulting residue was purified by column chromatography (PE/DCM/Tol/EtOH/NH_3 (33% aq sol) = 15:6:3:1:0.1) affording **1aB** as a yellow viscous oil. Yield = 50%. ^{1}H NMR (400 MHz, $CDCl_3$-*d*): δ 7.85–7.73 (m, 1H), 7.26–7.09 (m, 6H), 7.05–6.90 (m, 2H), 6.91–6.80 (m, 2H), 4.39 (bs, 1H), 4.05–3.95 (m, 2H), 3.79 (s, 3H), 3.78–3.73 (m, 2H), 2.92 (t, *J* = 6.5 Hz, 2H), 2.51 (t, *J* = 6.4 Hz, 2H), 1.79–1.64 (m, 2H), 1.62–1.48 (m, 2H). ^{13}C NMR (100 MHz, $CDCl_3$): δ 156.37, 156.14, 148.86, 144.90, 143.28, 130.31, 129.00, 128.19, 127.77, 127.42, 126.68, 123.21, 121.74, 120.38, 119.29, 115.82, 101.25, 55.39, 47.26, 44.77, 33.71, 24.25, 22.75. HRMS (ESI$^+$): $[M]^+$ = calculated for $C_{28}H_{28}N_3OS^+$ (*m*/*z*), 454.194 76; found, 454.194 76. LC-MS purity > 96%.

*6-Chloro-N-[2-(10H-phenothiazin-10-yl)ethyl]-1,2,3,4-tetrahydroacridin-9-amine (**1aC**).* The resulting residue was purified by column chromatography (PE/DCM/Tol/EtOH/NH_3 (33% aq sol) = 15:6:3:1:0.1) affording **1aC** as a yellow viscous oil. Yield = 42%. ^{1}H NMR (400 MHz, $CDCl_3$-*d*): δ 7.88–7.73 (m, 2H), 7.31–7.20 (m, 2H), 7.21–7.09 (m, 3H), 7.05–6.94 (m, 2H), 6.90–6.78 (m, 2H), 4.56 (bs, 1H), 4.11–3.96 (m, 2H), 3.85–3.72 (m, 2H), 2.92 (t, *J* = 6.5 Hz, 2H), 2.59–2.42 (m, 2H), 1.83–1.70 (m, 2H), 1.66–1.54 (m, 2H). ^{13}C NMR (100 MHz, $CDCl_3$): δ 159.92, 150.02, 144.75, 133.85, 128.99, 128.18, 127.82, 127.59, 127.45, 126.74, 124.47, 124.29, 123.30, 119.17, 118.33, 115.82, 47.22, 45.17, 33.98, 24.18, 22.62, 22.56. HRMS (ESI$^+$): $[M]^+$ = calculated for $C_{27}H_{25}N_3ClS^+$ (*m*/*z*), 458.145 22; found, 458.145 57. LC-MS purity > 98%.

*N-[2-(2-Chloro-10H-phenothiazin-10-yl)ethyl]-1,2,3,4-tetrahydroacridin-9-amine (**2aA**).* The resulting residue was purified by column chromatography (PE/DCM/Tol/EtOH/NH_3 (33% aq sol) = 15:6.5:3:0.5:0.05) affording **2aA** as a yellow viscous oil. Yield = 49%. ^{1}H NMR (400 MHz, $CDCl_3$-*d*): δ 7.88–7.81 (m, 2H), 7.56–7.45 (m, 1H), 7.32–7.19 (m, 2H), 7.20–7.07 (m, 2H), 7.07–6.93 (m, 2H), 6.84–6.80 (m, 2H), 4.45 (bs, 1H), 4.09–3.95 (m, 2H), 3.80 (t, *J* = 5.3 Hz, 2H), 2.97 (t, *J* = 6.5 Hz, 2H), 2.53 (t, *J* = 6.4 Hz, 2H), 1.86–1.70 (m, 2H), 1.69–1.56 (m, 2H). ^{13}C NMR (100 MHz, $CDCl_3$): δ 158.76, 149.64, 147.37, 146.15, 144.17, 133.46, 128.99, 128.82, 128.25, 127.83, 127.62, 126.34, 125.12, 123.89, 123.64, 123.09, 122.58, 120.88, 118.32, 116.25, 116.08, 47.48, 45.04, 34.02, 24.34, 22.76, 22.71. HRMS (ESI$^+$): $[M]^+$ = calculated for $C_{27}H_{25}ClN_3S^+$ (*m*/*z*), 458.145 22; found, 458.145 42. LC-MS purity > 99%.

*N-[2-(2-Chloro-10H-phenothiazin-10-yl)ethyl]-7-methoxy-1,2,3,4-tetrahydroacridin-9-amine (**2aB**).* The resulting residue was purified by column chromatography (PE/DCM/Tol/EtOH/NH_3 (33% aq sol) = 15:6.5:3:0.5:0.05) affording **2aB** as a yellow viscous oil. Yield = 41%. ^{1}H NMR (400 MHz, $CDCl_3$-*d*): δ 7.82–7.77 (m, 1H), 7.28–7.07 (m, 5H), 7.03–6.93 (m, 2H), 6.88–6.80 (m, 2H), 4.30 (bs, 1H), 3.99 (t, 2H), 3.81 (s, 3H), 3.78–3.73 (m, 2H), 2.93 (t, *J* = 6.5 Hz, 2H), 2.51 (t, *J* = 6.4 Hz, 2H), 1.82–1.67 (m, 2H), 1.64–1.50 (m, 2H). ^{13}C NMR (100 MHz, $CDCl_3$): δ 156.22, 148.58, 146.18, 144.22, 133.47, 130.40, 128.99, 128.25, 128.18, 127.82, 127.63, 126.33, 125.11, 123.64, 123.08, 121.73, 120.39, 119.32, 116.24, 116.07, 101.16, 55.42, 47.51, 44.62, 33.71, 24.30, 22.75, 22.75. HRMS (ESI$^+$): $[M]^+$ = calculated for $C_{28}H_{27}ClN_3OS^+$ (*m*/*z*), 488.155 79; found, 488.155 91. LC-MS purity > 98%.

*6-Chloro-N-[2-(2-chloro-10H-phenothiazin-10-yl)ethyl]-1,2,3,4-tetrahydroacridin-9-amine (**2aC**).* The resulting residue was purified by column chromatography (EA/DCM = 1:1) affording **2aC** as a yellow viscous oil. Yield = 64%. ^{1}H NMR (400 MHz, $CDCl_3$-*d*): δ 7.87–7.83 (m, 1H), 7.83–7.78 (m, 1H), 7.28–7.11 (m, 5H), 7.07–6.95 (m, 2H), 6.88–6.81 (m, 2H), 4.57–4.39 (m, 1H), 4.07–3.95 (m, 2H), 3.89–3.74 (m, 2H), 2.95 (t, *J* = 6.5 Hz, 2H), 2.51 (t, *J* = 6.4 Hz, 2H), 1.85–1.71 (m, 2H), 1.71–1.57 (m, 2H). ^{13}C NMR (100 MHz, $CDCl_3$): δ 159.97, 149.79, 147.91, 146.04, 144.07, 133.92, 133.51, 128.29, 127.87, 127.66, 126.37, 125.14, 124.58, 124.11, 123.72, 123.18, 119.16, 118.35, 116.25, 116.07, 109.99, 47.50, 45.03, 33.97, 24.26, 22.63, 22.56. HRMS (ESI$^+$): $[M]^+$ = calculated for $C_{27}H_{24}Cl_2N_3S^+$ (*m*/*z*), 492.106 25; found, 492.106 51. LC-MS purity > 97%.

*N-{2-[2-(Trifluoromethyl)-10H-phenothiazin-10-yl]ethyl}-1,2,3,4-tetrahydroacridin-9-amine (**3aA**).* The resulting residue was purified by column chromatography (PE/DCM/Tol/EtOH/NH_3 (33% aq sol) = 15:6.5:3:0.5:0.05) affording **3aA** as a yellow viscous oil. Yield = 32%. ^{1}H NMR (400 MHz, $CDCl_3$-*d*): δ 7.89–7.82 (m, 2H), 7.53–7.46 (m, 1H), 7.33–7.11 (m, 5H), 7.07–6.97 (m, 2H), 6.90–6.82 (m, 1H), 4.42 (s, 1H), 4.12–4.00 (m, 2H), 3.90–3.74 (m, 2H), 2.97

https://doi.org/10.1021/acschemneuro.1c00184
ACS Chem. Neurosci. 2021, 12, 1698–1715

(t, J = 6.5 Hz, 2H), 2.52 (t, J = 6.4 Hz, 2H), 1.89−1.69 (m, 2H), 1.68−1.52 (m, 2H). ^{13}C NMR (100 MHz, $CDCl_3$): δ 158.76, 149.58, 147.35, 145.38, 143.96, 131.52, 128.99, 128.83, 128.23, 128.18, 127.87, 125.58, 125.26, 123.94, 123.86, 122.48, 121.84, 120.90, 119.84, 118.36, 116.17, 112.27, 47.61, 44.98, 33.99, 24.35, 22.74, 22.69. HRMS (ESI$^+$): $[M]^+$ = calculated for $C_{28}H_{25}F_3N_3S^+$ (m/z), 492.171 58; found, 492.171 57. LC-MS purity > 99%.

*7-Methoxy-N-{2-[2-(trifluoromethyl)-10H-phenothiazin-10-yl]-ethyl}-1,2,3,4-tetrahydroacridin-9-amine (**3aB**).* The resulting residue was purified by column chromatography (PE/DCM/Tol/EtOH/NH_3 (33% aq sol) = 15:6.5:3:0.5:0.05) affording **3aB** as a yellow viscous oil. Yield = 29%. ^{1}H NMR (400 MHz, $CDCl_3$-d): δ 7.85−7.75 (m, 1H), 7.34−7.27 (m, 1H), 7.25−7.13 (m, 4H), 7.11−7.07 (m, 1H), 7.06−6.97 (m, 2H), 6.89−6.84 (m, 1H), 4.29 (bs, 1H), 4.11−4.01 (m, 2H), 3.80 (s, 3H), 3.76 (t, J = 6.4 Hz, 3H), 2.93 (t, J = 6.5 Hz, 2H), 2.49 (t, J = 6.4 Hz, 2H), 1.79−1.67 (m, 2H), 1.60−1.49 (m, 2H). ^{13}C NMR (100 MHz, $CDCl_3$): δ 156.25, 145.40, 143.99, 131.52, 130.32, 130.01, 128.99, 128.18, 127.87, 127.85, 125.57, 125.25, 123.86, 121.70, 120.38, 119.83, 116.15, 101.17, 47.65, 44.54, 33.62, 24.28, 22.71, 22.69. HRMS (ESI$^+$): $[M]^+$ = calculated for $C_{29}H_{27}F_3N_3OS^+$ (m/z), 522.182 14; found, 522.182 80. LC-MS purity > 96%.

*6-Chloro-N-{2-[2-(trifluoromethyl)-10H-phenothiazin-10-yl]-ethyl}-1,2,3,4-tetrahydroacridin-9-amine (**3aC**).* The resulting residue was purified by column chromatography (EA/DCM = 1:1) affording **3aC** as a yellow viscous oil. Yield = 34%. ^{1}H NMR (400 MHz, $CDCl_3$-d): δ 7.88−7.81 (m, 1H), 7.81−7.73 (m, 1H), 7.32−7.26 (m, 1H), 7.26−7.12 (m, 4H), 7.05−6.96 (m, 2H), 6.88−6.80 (m, 1H), 4.45 (bs, 1H), 4.10−4.01 (m, 2H), 3.87−3.74 (m, 2H), 2.93 (t, J = 6.5 Hz, 2H), 2.48 (t, J = 6.4 Hz, 2H), 1.84−1.68 (m, 2H), 1.67−1.54 (m, 2H). ^{13}C NMR (100 MHz, $CDCl_3$): δ 159.86, 149.80, 145.26, 143.82, 134.00, 131.52, 130.05, 129.72, 127.90, 127.56, 125.59, 124.63, 124.03, 123.94, 119.95, 119.91, 119.10, 118.32, 116.15, 112.32, 112.28, 112.24, 47.62, 44.96, 33.86, 24.25, 22.59, 22.50. HRMS (ESI$^+$): $[M]^+$ = calculated for $C_{28}H_{24}ClF_3N_3S^+$ (m/z), 526.1326; found, 526.132 63. LC-MS purity > 99%.

*N-[3-(10H-Phenothiazin-10-yl)propyl]-1,2,3,4-tetrahydroacridin-9-amine (**1bA**).* The resulting residue was purified by column chromatography (PE/DCM/Tol/EtOH/NH_3 (33% aq sol) = 15:5.5:3:1.5:0.1) affording **1bA** as a yellow viscous oil. Yield = 67%. ^{1}H NMR (400 MHz, $CDCl_3$-d): δ 7.91−7.82 (m, 1H), 7.78−7.71 (m, 1H), 7.54−7.44 (m, 1H), 7.26−7.19 (m, 1H), 7.19−7.08 (m, 4H), 6.96−6.88 (m, 2H), 6.84−6.77 (m, 2H), 3.97 (t, J = 6.2 Hz, 2H), 3.54 (t, J = 6.5 Hz, 2H), 2.99 (t, J = 6.4 Hz, 2H), 2.48 (t, J = 6.3 Hz, 2H), 2.13−2.03 (m, 2H), 1.87−1.78 (m, 2H), 1.79−1.68 (m, 2H). ^{13}C NMR (100 MHz, $CDCl_3$): δ 158.52, 150.15, 147.25, 145.03, 129.00, 128.71, 128.17, 127.62, 127.30, 125.95, 125.27, 123.76, 122.80, 122.27, 120.36, 116.71, 115.65, 45.80, 44.03, 33.96, 28.11, 24.72, 22.98, 22.72. HRMS (ESI$^+$): $[M]^+$ = calculated for $C_{28}H_{28}N_3S^+$ (m/z), 438.199 85; found, 438.199 71. LC-MS purity > 99%.

*7-Methoxy-N-[3-(10H-phenothiazin-10-yl)propyl]-1,2,3,4-tetrahydroacridin-9-amine (**1bB**).* The resulting residue was purified by column chromatography (PE/DCM/Tol/EtOH/NH_3 (33% aq sol) = 15:5.5:3:1.5:0.1) affording **1bB** as a yellow viscous oil. Yield = 68%. ^{1}H NMR (400 MHz, $CDCl_3$-d): δ 7.82−7.74 (m, 1H), 7.27−7.07 (m, 6H), 6.95−6.87 (m, 2H), 6.83−6.77 (m, 2H), 3.98 (t, J = 6.2 Hz, 2H), 3.81 (s, 3H), 3.50 (t, J = 6.5 Hz, 2H), 3.01−2.92 (m, 2H), 2.49 (t, J = 6.3 Hz, 2H), 2.14−2.05 (m, 2H), 1.89−1.77 (m, 2H), 1.78−1.68 (m, 2H). ^{13}C NMR (100 MHz, $CDCl_3$): δ 156.16, 156.02, 149.32, 145.00, 143.19, 130.21, 129.00, 128.19, 127.61, 127.28, 125.82, 125.26, 122.79, 121.25, 120.24, 117.80, 115.58, 101.19, 55.43, 45.71, 44.25, 33.65, 28.32, 24.58, 22.99, 22.77. HRMS (ESI$^+$): $[M]^+$ = calculated for $C_{29}H_{30}N_3OS^+$ (m/z), 468.210 41; found, 468.210 42. LC-MS purity > 98%.

*6-Chloro-N-[3-(10H-phenothiazin-10-yl)propyl]-1,2,3,4-tetrahydroacridin-9-amine (**1bC**).* The resulting residue was purified by column chromatography (EA/DCM = 1:1) affording **1bC** as a yellow viscous oil. Yield = 60%. ^{1}H NMR (400 MHz, $CDCl_3$-d): δ 7.87−7.76 (m, 1H), 7.68−7.61 (m, 1H), 7.18−7.08 (m, 5H), 6.97−6.89 (m, 2H), 6.84−6.77 (m, 2H), 3.98 (t, J = 6.1 Hz, 2H), 3.54 (t, J = 6.4 Hz, 2H), 2.94 (t, J = 6.4 Hz, 2H), 2.44 (t, J = 6.3 Hz, 2H), 2.08 (p, J = 6.3 Hz, 2H), 1.86−1.78 (m, 2H), 1.77−1.69 (m, 2H). ^{13}C NMR (100 MHz, $CDCl_3$): δ 159.61, 150.27, 147.88, 144.96, 133.83, 127.66, 127.56, 127.30, 126.06, 124.36, 123.99, 122.87, 118.56, 116.62, 115.65, 45.93, 43.95, 33.96, 28.08, 24.50, 22.85, 22.58. HRMS (ESI$^+$): $[M]^+$ = calculated for $C_{28}H_{27}ClN_3S^+$ (m/z), 472.160 87; found, 472.160 92. LC-MS purity > 99%.

*N-[3-(2-Chloro-10H-phenothiazin-10-yl)propyl]-1,2,3,4-tetrahydroacridin-9-amine (**2bA**).* The resulting residue was purified by column chromatography (PE/DCM/Tol/EtOH/NH_3 (33% aq sol) = 15:6.5:3:0.5:0.05) affording **2bA** as a yellow viscous oil. Yield = 29%. ^{1}H NMR (400 MHz, $CDCl_3$-d): δ 7.89−7.83 (m, 1H), 7.78−7.72 (m, 1H), 7.55−7.47 (m, 1H), 7.26−7.21 (m, 1H), 7.17−7.11 (m, 2H), 7.05−7.01 (m, 1H), 6.99−6.88 (m, 2H), 6.83−6.76 (m, 2H), 3.95 (t, J = 6.2 Hz, 2H), 3.56 (t, J = 6.4 Hz, 2H), 3.00 (t, J = 6.4 Hz, 2H), 2.53 (t, J = 6.3 Hz, 2H), 2.14−2.05 (m, 2H), 1.91−1.81 (m, 2H), 1.81−1.72 (m, 1H). ^{13}C NMR (100 MHz, $CDCl_3$): δ 150.08, 146.33, 144.26, 133.32, 128.99, 128.70, 128.25, 128.18, 128.09, 127.70, 127.48, 125.72, 125.26, 124.46, 123.85, 123.26, 122.66, 122.16, 116.69, 116.01, 115.94, 45.62, 44.11, 33.86, 28.09, 24.81, 22.96, 22.71. HRMS (ESI$^+$): $[M]^+$ = calculated for $C_{28}H_{27}ClN_3S^+$ (m/z), 472.160 87; found, 472.160 86. LC-MS purity > 96%.

*N-[3-(2-Chloro-10H-phenothiazin-10-yl)propyl]-7-methoxy-1,2,3,4-tetrahydroacridin-9-amine (**2bB**).* The resulting residue was purified by column chromatography (PE/DCM/Tol/EtOH/NH_3 (33% aq sol) = 15:6:3:1:0.1) affording **2bB** as a yellow viscous oil. Yield = 20%. ^{1}H NMR (400 MHz, $CDCl_3$-d): δ 7.83−7.73 (m, 1H), 7.27−7.05 (m, 4H), 7.03−6.97 (m, 1H), 6.97−6.84 (m, 2H), 6.82−6.72 (m, 2H), 3.95 (t, J = 6.2 Hz, 2H), 3.83 (s, 3H), 3.52 (t, J = 6.5 Hz, 2H), 2.97 (t, J = 6.4 Hz, 2H), 2.52 (t, J = 6.3 Hz, 2H), 2.19−2.04 (m, 2H), 1.90−1.79 (m, 2H), 1.79−1.70 (m, 2H). ^{13}C NMR (100 MHz, $CDCl_3$): δ 156.09, 149.42, 146.27, 144.24, 133.30, 129.91, 128.99, 128.06, 127.68, 127.46, 125.58, 124.32, 123.24, 122.63, 121.08, 120.34, 115.94, 115.86, 101.22, 55.45, 45.48, 44.32, 33.36, 28.30, 24.69, 22.94, 22.68. HRMS (ESI$^+$): $[M]^+$ = calculated for $C_{29}H_{29}ClN_3OS^+$ (m/z), 502.171 44; found, 502.171 39. LC-MS purity > 97%.

*6-Chloro-N-[3-(2-chloro-10H-phenothiazin-10-yl)propyl]-1,2,3,4-tetrahydroacridin-9-amine (**2bC**).* The resulting residue was purified by column chromatography (EA/DCM = 1:1) affording **2bC** as a yellow viscous oil. Yield = 26%. ^{1}H NMR (400 MHz, $CDCl_3$-d): δ 7.85−7.81 (m, 1H), 7.70−7.64 (m, 1H), 7.22−7.08 (m, 2H), 7.04−6.99 (m, 1H), 6.98−6.92 (m, 1H), 6.92−6.87 (m, 1H), 6.87−6.83 (m, 1H), 6.81−6.76 (m, 1H), 6.76−6.73 (m, 1H), 3.93 (t, J = 6.1 Hz, 2H), 3.57 (t, J = 6.4 Hz, 2H), 2.96 (t, J = 6.3 Hz, 2H), 2.47 (t, J = 6.2 Hz, 2H), 2.14−2.05 (m, 2H), 1.88−1.70 (m, 4H). ^{13}C NMR (100 MHz, $CDCl_3$): δ 159.32, 150.57, 146.22, 144.13, 134.21, 133.33, 129.47, 128.10, 127.73, 127.48, 126.96, 125.79, 124.53, 124.02, 123.35, 122.74, 119.58, 118.26, 115.99, 115.93, 115.59, 45.70, 43.98, 33.38, 28.07, 24.57, 22.75, 22.42. HRMS (ESI$^+$): $[M]^+$ = calculated for $C_{28}H_{26}Cl_2N_3S^+$ (m/z), 506.121 90; found, 506.122 01. LC-MS purity > 98%.

*N-{3-[2-(Trifluoromethyl)-10H-phenothiazin-10-yl]propyl}-1,2,3,4-tetrahydroacridin-9-amine (**3bA**).* The resulting residue was purified by column chromatography (PE/DCM/Tol/EtOH/NH_3 (33% aq sol) = 15:6:3:1:0.1) affording **3bA** as a yellow viscous oil. Yield = 40%. ^{1}H NMR (400 MHz, $CDCl_3$-d): δ 7.90−7.83 (m, 1H), 7.77−7.71 (m, 1H), 7.55−7.47 (m, 1H), 7.25−7.20 (m, 2H), 7.18−7.10 (m, 3H), 7.04−6.93 (m, 2H), 6.85−6.77 (m, 1H), 4.01 (t, J = 6.2 Hz, 2H), 3.56 (t, J = 6.5 Hz, 2H), 2.99 (t, J = 6.4 Hz, 2H), 2.52 (t, J = 6.3 Hz, 2H), 2.11 (p, J = 6.4 Hz, 2H), 1.89−1.79 (m, 2H), 1.80−1.70 (m, 2H). ^{13}C NMR (100 MHz, $CDCl_3$): δ 158.40, 150.14, 147.02, 145.47, 144.17, 130.91, 129.84, 129.52, 128.99, 128.57, 128.32, 128.18, 127.75, 127.73, 127.71, 125.26, 124.96, 123.89, 123.48, 122.12, 120.26, 119.48, 119.44, 116.69, 116.01, 112.11, 112.07, 45.65, 44.22, 33.72, 28.04, 24.78, 22.90, 22.64. HRMS (ESI$^+$): $[M]^+$ = calculated for $C_{29}H_{27}F_3N_3S^+$ (m/z), 506.187 23; found, 506.187 16. LC-MS purity > 96%.

*7-Methoxy-N-{3-[2-(trifluoromethyl)-10H-phenothiazin-10-yl]-propyl}-1,2,3,4-tetrahydroacridin-9-amine (**3bB**).* The resulting

https://doi.org/10.1021/acschemneuro.1c00184
ACS Chem. Neurosci. 2021, 12, 1698−1715

residue was purified by column chromatography (PE/DCM/Tol/EtOH/NH_3 (33% aq sol) = 15:5.5:3:1.5:1) affording **3bB** as a yellow viscous oil. Yield = 41%. ^{1}H NMR (400 MHz, $CDCl_3$-*d*): δ 7.81−7.74 (m, 1H), 7.28−7.10 (m, 5H), 7.10−7.07 (m, 1H), 7.02−6.92 (m, 2H), 6.84−6.77 (m, 1H), 4.01 (t, *J* = 6.2 Hz, 2H), 3.82 (s, 3H), 3.51 (t, *J* = 6.6 Hz, 2H), 2.96 (t, *J* = 6.4 Hz, 2H), 2.52 (t, *J* = 6.3 Hz, 2H), 2.11 (p, *J* = 6.4 Hz, 2H), 1.90−1.80 (m, 2H), 1.78−1.71 (m, 2H). ^{13}C NMR (100 MHz, $CDCl_3$): δ 156.11, 149.17, 145.40, 144.18, 130.22, 128.99, 128.18, 127.73, 127.71, 127.69, 125.25, 124.83, 123.45, 121.24, 120.25, 119.44, 117.87, 115.92, 112.06, 112.02, 109.99, 101.15, 55.40, 45.57, 44.46, 33.57, 28.25, 24.67, 22.94, 22.73. HRMS (ESI$^+$): [M]$^+$ = calculated for $C_{30}H_{29}F_3N_3OS^+$ (*m*/*z*), 536.197 79; found, 536.197 75. LC-MS purity > 98%.

*6-Chloro-N-{3-[2-(trifluoromethyl)-10H-phenothiazin-10-yl]-propyl}-1,2,3,4-tetrahydroacridin-9-amine (**3bC**).* The resulting residue was purified by column chromatography (EA/DCM = 1:1) affording **3bC** as a yellow viscous oil. Yield = 63%. ^{1}H NMR (400 MHz, $CDCl_3$-*d*): δ 7.82−7.79 (m, 1H), 7.70−7.63 (m, 1H), 7.23−7.08 (m, 5H), 7.01−6.92 (m, 2H), 6.83−6.77 (m, 1H), 4.00 (t, *J* = 6.1 Hz, 2H), 3.91 (bs, 1H), 3.54 (t, *J* = 6.5 Hz, 2H), 2.94 (t, *J* = 6.4 Hz, 2H), 2.48 (t, *J* = 6.3 Hz, 2H), 2.09 (p, *J* = 6.4 Hz, 2H), 1.89−1.79 (m, 2H), 1.78−1.70 (m, 2H). ^{13}C NMR (100 MHz, $CDCl_3$): δ 159.66, 150.13, 147.89, 145.39, 144.10, 133.88, 130.99, 129.83, 129.51, 127.78, 127.73, 127.63, 125.03, 124.45, 123.90, 123.54, 119.53, 119.49, 118.56, 116.72, 115.99, 112.10, 112.07, 45.79, 44.12, 33.92, 28.06, 24.57, 22.80, 22.55. HRMS (ESI$^+$): [M]$^+$ = calculated for $C_{29}H_{26}ClF_3N_3S^+$ (*m*/*z*), 540.148 26; found, 540.148 25. LC-MS > 98%.

*N-[4-(10H-Phenothiazin-10-yl)butyl]-1,2,3,4-tetrahydroacridin-9-amine (**1cA**).* The resulting residue was purified by column chromatography (PE/DCM/Tol/EtOH/NH_3 (33% aq sol) = 15:5.5:3:1.5:0.15) affording **1cA** as a dark yellow viscous oil. Yield = 74%. ^{1}H NMR (400 MHz, $CDCl_3$-*d*): δ 7.92−7.85 (m, 1H), 7.85−7.80 (m, 1H), 7.56−7.46 (m, 1H), 7.29−7.20 (m, 1H), 7.18−7.07 (m, 4H), 6.95−6.86 (m, 2H), 6.84−6.76 (m, 2H), 3.86 (t, *J* = 6.4 Hz, 2H), 3.45 (t, *J* = 6.9 Hz, 2H), 3.02 (t, *J* = 6.2 Hz, 2H), 2.54 (t, *J* = 6.1 Hz, 2H), 1.92−1.79 (m, 6H), 1.79−1.70 (m, 2H). ^{13}C NMR (100 MHz, $CDCl_3$): δ 158.44, 150.36, 147.46, 145.11, 128.76, 128.17, 127.57, 127.22, 125.48, 123.56, 122.66, 122.59, 120.14, 115.92, 115.53, 48.81, 46.67, 34.05, 29.00, 24.71, 24.16, 23.04, 22.75. HRMS (ESI$^+$): [M]$^+$ = calculated for $C_{29}H_{30}N_3S^+$ (*m*/*z*), 452.215 50; found, 452.215 27. LC-MS purity > 98%.

*7-Methoxy-N-[4-(10H-phenothiazin-10-yl)butyl]-1,2,3,4-tetrahydroacridin-9-amine (**1cB**).* The resulting residue was purified by column chromatography (PE/DCM/Tol/EtOH/NH_3 (33% aq sol) = 15:5.5:3:1.5:0.15) affording **1cB** as a dark yellow viscous oil. Yield = 57%. ^{1}H NMR (400 MHz, $CDCl_3$-*d*): δ 7.83−7.77 (m, 1H), 7.23−7.18 (m, 1H), 7.15−7.07 (m, 5H), 6.93−6.86 (m, 2H), 6.83−6.77 (m, 2H), 3.87 (t, *J* = 6.5 Hz, 2H), 3.80 (s, 3H), 3.38 (t, *J* = 7.0 Hz, 2H), 3.00 (t, *J* = 6.1 Hz, 2H), 2.58 (t, *J* = 6.0 Hz, 2H), 1.94−1.80 (m, 6H), 1.79−1.70 (m, 2H). ^{13}C NMR (100 MHz, $CDCl_3$): δ 156.15, 155.87, 149.50, 145.11, 143.38, 130.27, 127.55, 127.19, 125.47, 122.58, 121.20, 120.27, 117.40, 115.49, 101.47, 55.39, 48.58, 46.72, 33.78, 29.00, 24.64, 24.35, 23.05, 22.80. HRMS (ESI$^+$): [M]$^+$ = calculated for $C_{30}H_{32}N_3OS^+$ (*m*/*z*), 482.226 06; found, 482.225 83. LC-MS purity > 99%.

*6-Chloro-N-[4-(10H-phenothiazin-10-yl)butyl]-1,2,3,4-tetrahydroacridin-9-amine (**1cC**).* The resulting residue was purified by column chromatography (EA/DCM = 1:1) affording **1cC** as a yellow sticky foam. Yield = 61%. ^{1}H NMR (400 MHz, $CDCl_3$-*d*): δ 7.86−7.81 (m, 1H), 7.76−7.70 (m, 1H), 7.17−7.06 (m, 5H), 6.93−6.86 (m, 2H), 6.82−6.76 (m, 2H), 3.87 (t, *J* = 6.3 Hz, 2H), 3.44 (t, *J* = 6.9 Hz, 2H), 2.98 (t, *J* = 6.1 Hz, 2H), 2.47 (t, *J* = 6.0 Hz, 2H), 1.90−1.78 (m, 6H), 1.78−1.69 (m, 2H). ^{13}C NMR (100 MHz, cdcl$_3$): δ 159.46, 150.42, 148.06, 145.08, 133.84, 127.60, 127.53, 127.21, 125.58, 124.39, 124.14, 122.64, 118.27, 115.74, 115.55, 48.85, 46.55, 34.00, 28.97, 24.46, 24.02, 22.90, 22.59. HRMS (ESI$^+$): [M]$^+$ = calculated for $C_{29}H_{29}ClN_3S^+$ (*m*/*z*), 486.176 52; found, 486.176 36. LC-MS purity > 97%.

*N-[4-(2-Chloro-10H-phenothiazin-10-yl)butyl]-1,2,3,4-tetrahydroacridin-9-amine (**2cA**).* The resulting residue was purified by column chromatography (EA/DCM = 1:1) affording **2cA** as a yellow viscous oil. Yield = 50%. ^{1}H NMR (400 MHz, $CDCl_3$-*d*): δ 7.90−7.76 (m, 2H), 7.57−7.47 (m, 1H), 7.30−7.22 (m, 1H), 7.15−7.06 (m, 2H), 7.03−6.97 (m, 1H), 6.96−6.83 (m, 2H), 6.82−6.74 (m, 2H), 3.84 (t, *J* = 6.3 Hz, 2H), 3.45 (t, *J* = 6.9 Hz, 2H), 3.02 (t, *J* = 6.1 Hz, 2H), 2.55 (t, *J* = 6.0 Hz, 2H), 1.92−1.80 (m, 6H), 1.79−1.69 (m, 2H). ^{13}C NMR (100 MHz, $CDCl_3$): δ 158.39, 150.31, 147.38, 146.41, 144.37, 133.21, 128.72, 128.22, 128.03, 127.64, 127.40, 125.25, 123.61, 123.06, 122.60, 122.43, 120.11, 115.95, 115.87, 115.84, 109.99, 48.76, 46.82, 34.01, 28.92, 24.72, 24.04, 23.02, 22.73. HRMS (ESI$^+$): [M]$^+$ = calculated for $C_{29}H_{29}ClN_3S^+$ (*m*/*z*), 486.176 52; found, 486.176 33. LC-MS purity > 98%.

*N-[4-(2-Chloro-10H-phenothiazin-10-yl)butyl]-7-methoxy-1,2,3,4-tetrahydroacridin-9-amine (**2cB**).* The resulting residue was purified by column chromatography (PE/DCM/Tol/EtOH/NH_3 (33% aq sol) = 15:5.5:3:1.5:0.15) affording **2cB** as a yellow viscous oil. Yield = 50%. ^{1}H NMR (400 MHz, $CDCl_3$-*d*): δ 7.83−7.76 (m, 1H), 7.23−7.17 (m, 1H), 7.15−7.08 (m, 3H), 7.02−6.96 (m, 1H), 6.95−6.88 (m, 1H), 6.88−6.84 (m, 1H), 6.81−6.76 (m, 2H), 3.88−3.76 (m, 5H), 3.38 (t, *J* = 7.0 Hz, 2H), 3.00 (t, *J* = 6.0 Hz, 2H), 2.59 (t, *J* = 5.9 Hz, 2H), 1.93−1.79 (m, 6H), 1.80−1.69 (m, 2H). ^{13}C NMR (100 MHz, $CDCl_3$): δ 156.11, 155.90, 149.46, 146.41, 144.38, 143.28, 133.19, 130.19, 128.01, 127.62, 127.39, 125.24, 123.99, 123.05, 122.42, 121.18, 120.30, 117.39, 115.84, 115.81, 101.46, 55.40, 48.52, 46.87, 33.70, 28.92, 24.66, 24.22, 23.03, 22.78. HRMS (ESI$^+$): [M]$^+$ = calculated for $C_{30}H_{31}ClN_3OS^+$ (*m*/*z*), 516.187 09; found, 516.187 01. LC-MS purity > 97%.

*6-Chloro-N-[4-(2-chloro-10H-phenothiazin-10-yl)butyl]-1,2,3,4-tetrahydroacridin-9-amine (**2cC**).* The resulting residue was purified by column chromatography (EA/DCM = 1:1) affording **2cC** as a yellow viscous oil. Yield = 47%. ^{1}H NMR (400 MHz, $CDCl_3$-*d*): δ 7.86−7.81 (m, 1H), 7.76−7.71 (m, 1H), 7.18−7.08 (m, 3H), 7.02−6.96 (m, 1H), 6.95−6.89 (m, 1H), 6.89−6.84 (m, 1H), 6.81−6.74 (m, 2H), 3.84 (t, *J* = 6.2 Hz, 2H), 3.45 (t, *J* = 6.9 Hz, 2H), 2.98 (t, *J* = 6.0 Hz, 2H), 2.49 (t, *J* = 6.0 Hz, 2H), 1.92−1.78 (m, 6H), 1.78−1.68 (m, 2H). ^{13}C NMR (100 MHz, $CDCl_3$): δ 159.40, 150.38, 147.95, 146.34, 144.34, 133.92, 133.21, 128.05, 127.66, 127.48, 127.40, 125.32, 124.32, 124.20, 124.08, 123.10, 122.47, 118.23, 115.89, 115.84, 115.76, 48.80, 46.70, 33.93, 28.88, 24.48, 23.90, 22.88, 22.56. HRMS (ESI$^+$): [M]$^+$ = calculated for $C_{29}H_{28}Cl_2N_3S^+$ (*m*/*z*), 520.137 55; found, 520.137 33. LC-MS purity > 97%.

*N-{4-[2-(Trifluoromethyl)-10H-phenothiazin-10-yl]butyl}-1,2,3,4-tetrahydroacridin-9-amine (**3cA**).* The resulting residue was purified by column chromatography (PE/DCM/Tol/EtOH/NH_3 (33% aq sol)= 15:5.5:3:1.5:0.1) affording **3cA** as a yellow viscous oil. Yield = 63%. ^{1}H NMR (400 MHz, $CDCl_3$-*d*): δ 7.89−7.80 (m, 2H), 7.55−7.47 (m, 1H), 7.29−7.22 (m, 1H), 7.22−7.16 (m, 1H), 7.17−7.10 (m, 3H), 7.01−6.98 (m, 1H), 6.98−6.91 (m, 1H), 6.84−6.79 (m, 1H), 3.91 (t, *J* = 6.4 Hz, 2H), 3.84 (bs, 1H), 3.52−3.41 (m, 2H), 3.02 (t, *J* = 6.1 Hz, 2H), 2.57 (t, *J* = 6.1 Hz, 2H), 1.95−1.71 (m, 8H). ^{13}C NMR (100 MHz, $CDCl_3$): δ 158.50, 150.23, 147.49, 145.65, 144.17, 128.84, 128.18, 127.71, 127.62, 124.57, 123.61, 123.28, 122.53, 120.19, 119.25, 119.21, 116.08, 115.93, 111.95, 111.91, 48.79, 46.90, 34.07, 28.93, 24.74, 24.05, 23.01, 22.74. HRMS (ESI$^+$): [M]$^+$ = calculated for $C_{30}H_{29}F_3N_3S^+$ (*m*/*z*), 520.202 88; found, 520.202 64. LC-MS purity > 98%.

*7-Methoxy-N-{4-[2-(trifluoromethyl)-10H-phenothiazin-10-yl]-butyl}-1,2,3,4-tetrahydroacridin-9-amine (**3cB**).* The resulting residue was purified by column chromatography (PE/DCM/Tol/EtOH/NH_3 (33% aq sol) = 15:5.5:3:1.5:1) affording **3cB** as a yellow viscous oil. Yield = 53%. ^{1}H NMR (400 MHz, $CDCl_3$-*d*): δ 7.84−7.78 (m, 1H), 7.23−7.07 (m, 6H), 7.01−6.97 (m, 1H), 6.97−6.90 (m, 1H), 6.84−6.78 (m, 1H), 3.90 (t, *J* = 6.5 Hz, 2H), 3.80 (s, 3H), 3.38 (t, *J* = 7.0 Hz, 2H), 3.00 (t, *J* = 6.0 Hz, 2H), 2.59 (t, *J* = 6.0 Hz, 2H), 1.94−1.80 (m, 6H), 1.79−1.71 (m, 2H). ^{13}C NMR (100 MHz, $CDCl_3$): δ 156.11, 155.93, 149.50, 145.63, 144.18, 143.19, 130.46, 130.09, 129.73, 129.41, 127.69, 127.61, 124.54, 123.28, 121.19, 120.33, 119.23, 119.20, 117.41, 115.91, 111.92, 111.88, 101.45, 55.36, 48.51,

https://doi.org/10.1021/acschemneuro.1c00184
ACS Chem. Neurosci. 2021, 12, 1698−1715

46.94, 33.57, 28.91, 24.66, 24.19, 22.99, 22.74. HRMS (ESI$^+$): [M]$^+$ = calculated for $C_{31}H_{31}F_3N_3OS^+$ (m/z), 550.213 44; found, 550.213 01. LC-MS purity > 95%.

*6-Chloro-N-{4-[2-(trifluoromethyl)-10H-phenothiazin-10-yl]-butyl}-1,2,3,4-tetrahydroacridin-9-amine (**3cC**).* The resulting residue was purified by column chromatography (EA/DCM = 1:1) affording **3cC** as a yellow viscous oil. Yield = 52%. ^{1}H NMR (400 MHz, $CDCl_3$-*d*): δ 7.87−7.81 (m, 1H), 7.76−7.71 (m, 1H), 7.21−7.09 (m, 5H), 7.01−6.97 (m, 1H), 6.97−6.90 (m, 1H), 6.83−6.77 (m, 1H), 3.91 (t, J = 6.3 Hz, 2H), 3.45 (t, J = 6.9 Hz, 2H), 2.98 (t, J = 6.0 Hz, 2H), 2.50 (t, J = 6.0 Hz, 2H), 1.94−1.80 (m, 6H), 1.79−1.70 (m, 2H). ^{13}C NMR (100 MHz, $CDCl_3$): δ 159.47, 150.33, 148.01, 145.60, 144.14, 133.91, 130.53, 127.73, 127.64, 127.62, 127.55, 124.63, 124.26, 124.22, 123.32, 119.27, 119.23, 118.29, 115.93, 115.87, 111.96, 111.92, 48.83, 46.78, 33.97, 28.88, 24.48, 23.91, 22.86, 22.56. HRMS (ESI$^+$): [M]$^+$ = calculated for $C_{30}H_{28}ClF_3N_3S^+$ (m/z), 554.163 91; found, 554.163 64. LC-MS purity > 98%.

*N-[5-(10H-Phenothiazin-10-yl)pentyl]-1,2,3,4-tetrahydroacridin-9-amine (**1dA**).* The resulting residue was purified by column chromatography (PE/DCM/Tol/EtOH/NH_3 (25% aq sol) = 15:5.5:3:1.2:0.1) affording **1dA** as a yellow viscous oil. Yield = 78%. ^{1}H NMR (500 MHz, $CDCl_3$-*d*): δ 7.96−7.87 (m, 2H), 7.58−7.51 (m, 1H), 7.36−7.27 (m, 1H), 7.21−7.10 (m, 4H), 6.96−6.88 (m, 2H), 6.88−6.81 (m, 2H), 5.30 (bs, 1H), 3.88 (t, J = 6.7 Hz, 2H), 3.45 (t, J = 7.1 Hz, 2H), 3.06 (t, J = 6.1 Hz, 2H), 2.65 (t, J = 5.9 Hz, 2H), 1.97−1.78 (m, 6H), 1.72−1.61 (m, 2H), 1.61−1.48 (m, 2H). ^{13}C NMR (126 MHz, $CDCl_3$): δ 158.34, 150.65, 147.31, 145.22, 128.60, 128.25, 127.50, 127.16, 125.30, 123.58, 122.74, 122.47, 120.15, 115.90, 115.47, 49.28, 46.91, 33.89, 31.25, 26.45, 24.75, 24.24, 23.02, 22.72. HRMS (ESI$^+$): [M]$^+$ = calculated for $C_{30}H_{32}N_3S^+$ (m/z), 466.231 15; found, 466.230 74. LC-MS purity > 96%.

*7-Methoxy-N-[5-(10H-phenothiazin-10-yl)pentyl]-1,2,3,4-tetrahydroacridin-9-amine (**1dB**).* The resulting residue was purified by column chromatography (PE/DCM/Tol/EtOH/NH_3 (25% aq sol) = 15:5.5:3:1.2:0.1) affording **1 dB** as a yellow viscous oil. Yield = 45%. ^{1}H NMR (500 MHz, $CDCl_3$-*d*): δ 7.89−7.84 (m, 1H), 7.26−7.22 (m, 1H), 7.20−7.10 (m, 5H), 6.95−6.88 (m, 2H), 6.86−6.80 (m, 2H), 3.91−3.81 (m, 5H), 3.37 (t, J = 7.1 Hz, 2H), 3.04 (t, J = 6.0 Hz, 2H), 2.66 (t, J = 5.9 Hz, 2H), 1.94−1.77 (m, 6H), 1.70−1.60 (m, 2H), 1.58−1.48 (m, 2H). ^{13}C NMR (126 MHz, $CDCl_3$): δ 155.87, 155.78, 149.80, 145.11, 142.95, 129.84, 127.40, 127.09, 125.16, 122.38, 121.05, 120.28, 117.08, 115.38, 101.55, 55.32, 48.85, 46.82, 33.44, 31.20, 26.42, 24.57, 24.25, 22.92, 22.65. HRMS (ESI$^+$): [M]$^+$ = calculated for $C_{31}H_{34}N_3OS^+$ (m/z), 496.241 71; found, 496.241 21. LC-MS purity > 97%.

*6-Chloro-N-[5-(10H-phenothiazin-10-yl)pentyl]-1,2,3,4-tetrahydroacridin-9-amine (**1dC**).* The resulting residue was purified by column chromatography (EA/DCM = 1:1) affording **1dC** as a yellow viscous oil. Yield = 43%. ^{1}H NMR (500 MHz, $CDCl_3$-*d*): δ 7.94−7.87 (m, 1H), 7.86−7.79 (m, 1H), 7.25−7.20 (m, 1H), 7.20−7.11 (m, 4H), 6.92 (t, J = 7.4 Hz, 2H), 6.89−6.81 (m, 3H), 3.87 (t, J = 6.6 Hz, 2H), 3.42 (t, J = 7.0 Hz, 2H), 3.01 (t, J = 5.9 Hz, 2H), 2.58 (t, J = 5.6 Hz, 2H), 1.95−1.77 (m, 6H), 1.68−1.59 (m, 2H), 1.57−1.46 (m, 2H). ^{13}C NMR (126 MHz, $CDCl_3$): δ 159.36, 150.62, 147.94, 145.13, 133.83, 127.45, 127.36, 127.13, 125.24, 124.48, 124.07, 122.43, 118.23, 115.64, 115.45, 49.28, 46.76, 33.83, 31.16, 26.28, 24.46, 24.11, 22.82, 22.52. HRMS (ESI$^+$): [M]$^+$ = calculated for $C_{30}H_{31}ClN_3S^+$ (m/z), 500.192 17; found, 500.191 83. LC-MS purity > 96%.

*N-[5-(2-Chloro-10H-phenothiazin-10-yl)pentyl]-1,2,3,4-tetrahydroacridin-9-amine (**2dA**).* The resulting residue was purified by column chromatography (PE/DCM/Tol/EtOH/NH_3 (25% aq sol) = 15:5.5:3:1.2:0.1) affording **2dA** as a yellow viscous oil. Yield = 71%. ^{1}H NMR (500 MHz, $CDCl_3$-*d*): δ 7.97−7.87 (m, 2H), 7.57−7.51 (m, 1H), 7.35−7.27 (m, 1H), 7.17−7.09 (m, 2H), 7.03−6.98 (m, 1H), 6.96−6.90 (m, 1H), 6.90−6.85 (m, 1H), 6.85−6.78 (m, 2H), 3.82 (t, J = 6.7 Hz, 2H), 3.44 (t, J = 7.1 Hz, 2H), 3.06 (t, J = 6.0 Hz, 2H), 2.63 (t, J = 5.9 Hz, 2H), 1.95−1.84 (m, 4H), 1.84−1.76 (m, 2H), 1.69−1.60 (m, 2H), 1.55−1.46 (m, 2H). ^{13}C NMR (126 MHz, $CDCl_3$): δ 158.12, 150.65, 147.01, 146.41, 144.36, 133.08, 128.30, 128.26, 127.86, 127.47, 127.29, 124.92, 123.69, 123.53, 122.86, 122.67, 122.20, 119.96, 115.72, 115.67, 49.12, 46.92, 33.60, 31.11, 26.21, 24.65, 24.05, 22.90, 22.58. HRMS (ESI$^+$): [M]$^+$ = calculated for $C_{30}H_{31}ClN_3S^+$ (m/z), 500.192 17; found, 500.191 62. LC-MS purity > 95%.

*N-[5-(2-Chloro-10H-phenothiazin-10-yl)pentyl]-7-methoxy-1,2,3,4-tetrahydroacridin-9-amine (**2dB**).* The resulting residue was purified by column chromatography (PE/DCM/Tol/EtOH/NH_3 (25% aq sol) = 15:5.5:3:1.2:0.1) affording **2dB** as a yellow viscous oil. Yield = 39%. ^{1}H NMR (500 MHz, $CDCl_3$-*d*): δ 7.88−7.82 (m, 1H), 7.26−7.21 (m, 1H), 7.20−7.09 (m, 3H), 7.03−6.98 (m, 1H), 6.96−6.90 (m, 1H), 6.89−6.86 (m, 1H), 6.85−6.79 (m, 2H), 3.86 (s, 3H), 3.83 (t, J = 6.7 Hz, 2H), 3.37 (t, J = 7.1 Hz, 2H), 3.03 (t, J = 6.0 Hz, 2H), 2.66 (t, J = 5.8 Hz, 2H), 1.93−1.85 (m, 4H), 1.85−1.78 (m, 2H), 1.70−1.61 (m, 2H), 1.58−1.49 (m, 2H). ^{13}C NMR (126 MHz, $CDCl_3$): δ 155.86, 149.79, 146.44, 144.41, 142.96, 133.11, 129.87, 127.90, 127.51, 127.31, 124.96, 123.73, 122.89, 122.24, 121.08, 120.30, 117.13, 115.74, 115.72, 101.60, 55.37, 48.86, 47.00, 33.45, 31.20, 26.35, 24.63, 24.22, 22.96, 22.68. HRMS (ESI$^+$): [M]$^+$ = calculated for $C_{31}H_{33}ClN_3OS^+$ (m/z), 530.202 74; found, 530.202 33. LC-MS purity > 96%.

*6-Chloro-N-[5-(2-chloro-10H-phenothiazin-10-yl)pentyl]-1,2,3,4-tetrahydroacridin-9-amine (**2dC**).* The resulting residue was purified by column chromatography (EA/DCM = 1:1) affording **2dC** as a yellow viscous oil. Yield = 45%. ^{1}H NMR (500 MHz, $CDCl_3$-*d*): δ 7.90−7.86 (m, 1H), 7.84−7.79 (m, 1H), 7.25−7.20 (m, 1H), 7.18−7.09 (m, 2H), 7.03−6.98 (m, 1H), 6.96−6.90 (m, 1H), 6.90−6.86 (m, 1H), 6.84−6.78 (m, 2H), 3.83 (t, J = 6.6 Hz, 2H), 3.41 (t, J = 7.1 Hz, 2H), 3.05−2.96 (m, 2H), 2.64−2.54 (m, 2H), 1.93−1.85 (m, 4H), 1.85−1.75 (m, 2H), 1.68−1.59 (m, 2H), 1.55−1.47 (m, 2H). ^{13}C NMR (126 MHz, $CDCl_3$): δ 159.41, 150.54, 148.00, 146.42, 144.39, 133.84, 133.13, 127.90, 127.52, 127.43, 127.33, 124.99, 124.43, 124.11, 123.76, 122.92, 122.88, 122.26, 118.29, 115.77, 115.75, 49.27, 46.91, 33.91, 31.14, 26.20, 24.49, 24.05, 22.84, 22.55. HRMS (ESI$^+$): [M]$^+$ = calculated for $C_{29}H_{27}Cl_2N_3S^+$ (m/z), 534.153 20; found, 534.152 95. LC-MS purity > 98%.

*N-{5-[2-(Trifluoromethyl)-10H-phenothiazin-10-yl]pentyl}-1,2,3,4-tetrahydroacridin-9-amine (**3dA**).* The resulting residue was purified by column chromatography (PE/DCM/Tol/EtOH/NH_3 (25% aq sol) = 15:5.5:3:1.2:0.1) affording **3dA** as a yellow viscous oil. Yield = 64%. ^{1}H NMR (500 MHz, $CDCl_3$-*d*): δ 7.96−7.87 (m, 2H), 7.57−7.52 (m, 1H), 7.35−7.29 (m, 1H), 7.20−7.10 (m, 4H), 7.03−7.00 (m, 1H), 6.98−6.92 (m, 1H), 6.86−6.81 (m, 1H), 3.88 (t, J = 6.7 Hz, 2H), 3.44 (t, J = 7.1 Hz, 2H), 3.06 (t, J = 6.0 Hz, 2H), 2.64 (t, J = 6.0 Hz, 2H), 1.94−1.86 (m, 4H), 1.82 (p, J = 7.0 Hz, 2H), 1.70−1.60 (m, 2H), 1.58−1.49 (m, 2H). ^{13}C NMR (126 MHz, $CDCl_3$): δ 158.24, 150.58, 147.17, 145.58, 144.24, 128.44, 128.24, 127.54, 127.46, 124.22, 123.54, 123.09, 122.65, 120.04, 119.04, 119.01, 115.80, 115.78, 111.81, 111.78, 49.15, 47.02, 33.73, 31.15, 26.22, 24.67, 24.08, 22.92, 22.62. HRMS (ESI$^+$): [M]$^+$ = calculated for $C_{31}H_{31}F_3N_3S^+$ (m/z), 534.218 53; found, 534.218 08. LC-MS purity > 99%.

*7-Methoxy-N-{5-[2-(trifluoromethyl)-10H-phenothiazin-10-yl]-pentyl}-1,2,3,4-tetrahydroacridin-9-amine (**3dB**).* The resulting residue was purified by column chromatography (PE/DCM/Tol/EtOH/NH_3 (25% aq sol) = 15:5.5:3:1.2:0.1) affording **3dB** as a yellow viscous oil. Yield = 78%. ^{1}H NMR (500 MHz, $CDCl_3$-*d*): δ 7.88−7.84 (m, 1H), 7.26−7.21 (m, 1H), 7.21−7.10 (m, 5H), 7.03−6.99 (m, 1H), 6.99−6.92 (m, 1H), 6.88−6.81 (m, 1H), 3.89 (t, J = 6.7 Hz, 2H), 3.86 (s, 3H), 3.39 (t, J = 7.1 Hz, 2H), 3.03 (t, J = 6.2 Hz, 2H), 2.66 (t, J = 5.8 Hz, 2H), 1.92−1.78 (m, 6H), 1.67 (p, J = 7.4 Hz, 2H), 1.60−1.50 (m, 2H). ^{13}C NMR (126 MHz, $CDCl_3$): δ 155.90, 155.73, 149.94, 145.60, 144.28, 142.63, 130.19, 129.64, 129.60, 127.58, 127.56, 127.50, 124.25, 123.12, 120.97, 120.41, 119.07, 119.04, 119.01, 116.90, 115.80, 111.82, 111.79, 111.76, 101.64, 55.35, 48.81, 47.07, 33.25, 31.23, 26.33, 24.63, 24.22, 22.92, 22.60. HRMS (ESI$^+$): [M]$^+$ = calculated for $C_{32}H_{33}F_3N_3OS^+$ (m/z), 564.229 09; found, 564.228 33. LC-MS purity > 97%.

*6-Chloro-N-{5-[2-(trifluoromethyl)-10H-phenothiazin-10-yl]-pentyl}-1,2,3,4-tetrahydroacridin-9-amine (**3dC**).* The resulting residue was purified by column chromatography (EA/DCM = 1:1)

https://doi.org/10.1021/acschemneuro.1c00184
ACS Chem. Neurosci. 2021, 12, 1698−1715

affording **3dC** as a yellow viscous oil. Yield = 33%. ^{1}H NMR (500 MHz, $CDCl_3$-*d*): δ 7.92−7.89 (m, 1H), 7.84−7.80 (m, 1H), 7.25−7.11 (m, 5H), 7.04−7.00 (m, 1H), 6.99−6.93 (m, 1H), 6.88−6.84 (m, 1H), 3.90 (t, J = 6.6 Hz, 2H), 3.44 (t, J = 7.1 Hz, 2H), 3.05−2.98 (m, 2H), 2.64−2.55 (m, 2H), 1.94−1.78 (m, 6H), 1.66 (p, J = 7.0 Hz, 2H), 1.59−1.48 (m, 2H). ^{13}C NMR (126 MHz, $CDCl_3$): δ 159.32, 150.67, 147.81, 145.59, 144.27, 133.98, 130.22, 129.62, 129.37, 128.96, 128.25, 128.15, 127.61, 127.58, 127.52, 127.28, 124.43, 124.29, 124.17, 123.16, 119.11, 119.07, 118.19, 115.84, 115.61, 111.86, 111.83, 49.27, 46.98, 33.71, 31.18, 26.17, 24.47, 24.06, 22.81, 22.49. HRMS (ESI$^+$): $[M]^+$ = calculated for $C_{31}H_{30}ClF_3N_3S^+$ (m/z), 568.179 56; found, 568.179 56. LC-MS purity > 97%.

Biology. *Primary Rat CGNs.* CGNs were prepared from 7-day-old Wistar rats as described[31] and plated at the density of 1.2 × 10^5 cells/well on 96-well plates previously coated with 10 μg/mL poly L-lysine (Sigma-Aldrich, Milano, Italy). The medium used for the culture was BME with 10% heat-inactivated Fetal bovine serum (FBS, Aurogene, Rome, Italy), 2 mM glutamine (Aurogene, Rome, Italy), 100 μM gentamicin sulfate (Sigma-Aldrich, Milano, Italy), and 25 mM Potassium chloride (KCl, Sigma-Aldrich, Milano, Italy). After 16 h, 10 μM cytosine arabino-furanoside (Sigma-Aldrich, Milano, Italy) was added to avoid glial proliferation. After 7 days *in vitro*, the cells were exposed to compounds **1dC** and **2dC** at different concentrations (0, 0.5, 1, 2, and 5 μM) in serum-free BME medium. Cell viability was evaluated by MTT assay after 24 h of treatment. Statistical data analysis was performed through GraphPad Prism 4 by using one-way ANOVA followed by Bonferroni's posthoc comparison test.

Live Cell Counting after Hoechst Staining. Differentiated CGNs were exposed to **1dC** and **2dC** compounds at 5 μM for 24 h in serum-free medium. Cells were fixed for 20 min with 4% PFA in phosphate buffer, washed in PBS, and incubated with 0.1 μg/mL of Hoechst 33258 (Sigma-Aldrich, Milano, Italy) for 5 min at room temperature. Five randomly fields were acquired from each sample by using a fluorescence microscope (20× objective; Nikon Eclipse TE 2000-S microscope, equipped with an AxioCam MRm digital camera). Live cells were counted by using the manual cell counter plugin of Fiji ImageJ2 software.

$\tau_{(306-336)}$ Pretreatment. $\tau_{(306-336)}$ (1 mg) (Bachem AG, Weil am Rhein, Germany) was initially dissolved in 1,1,1,3,3,3,-hexafluoro-2-propanol (HFIP), gently vortexed, sonicated, and kept overnight at room temperature. Subsequently, the sample was aliquoted, dried, and stored at −20 °C.

$\tau_{(306-336)}$ Peptide Aggregation and Its Inhibition by ThT Fluorimetric Assay. Stock solutions of $\tau_{(306-336)}$ peptide (500 μM) were prepared in ultrapure water and immediately used. Stock solution of ThT (500 μM) was prepared in 56.3 mM phosphate buffer (PB, pH = 7.4), while stock solutions of inhibitors (20 mM) and of the reference compounds tacrine and phenothiazine (10 mM) were prepared in DMSO/methanol 10/90. $\tau_{(306-336)}$ aggregation was monitored at 30 °C in a black, clear-bottom 96-well plate (Greiner) by EnSpire multiplate reader (PerkinElmer, Waltham, Massachusetts, USA) using ThT fluorimetric assay[14] with some variations. The excitation and emission wavelengths were set at 446 and 490 nm, respectively. Assay samples were prepared by diluting $\tau_{(306-336)}$ stock solution to 50 μM in the assay mixture which consisted in 20 μM ThT, 48.1 mM PB (final concentrations) in a final 100 μL volume (final DMSO and MeOH content: 0.05% and 0.45%, respectively). Inhibition experiments were performed by incubating $\tau_{(306-336)}$ peptide at the given conditions in the presence of tested inhibitors at 50 μM. Fluorescence data were recorded every 10 min overnight with 1 min of shaking at 800 rpm prior to each reading. Each inhibitor was assayed in triplicate in at least two independent experiments. Estimation of the inhibitory potency (%) was carried out by comparing fluorescence values at the plateau (average fluorescence intensity value in the 12−16 h range). Inhibition % values are expressed as the mean ± SEM. Quenching of ThT fluorescence was evaluated by preparing blank solutions containing inhibitor/reference compound and preformed fibrils of $\tau_{(306-336)}$ peptide.

Aβ_{1-42} Inhibition Assay. Stock solutions of tested inhibitors were prepared in DMSO and diluted in 10 mM PBS containing 150 mM NaCl (pH = 8) to the final concentration in the well (50 μM). Thioflavin T (ThT, final concentration 20 μM) was added to the well after it was dissolved in methanol and subsequently diluted in 50 mM glycine−NaOH (pH = 8.6) to 0.4 mM. Finally, Aβ_{1-42} (HFIP-treated, BACHEM) was added to reach the 50 μM final concentration per well. Initially, 1 mg of Aβ_{1-42} was dissolved in DMSO to obtain the stock solution and stored at −20 °C. Before the assay, Aβ_{1-42} stock solution was briefly sonicated and vortexed and added to the 96-well plate as the last component. The final volume of the assay mixture was 100 μL. Aβ_{1-42} self-aggregation was performed at room temperature without any stirring in a black, clear-bottom 96-well plate (Greiner) by a multiplate reader (Synergy HT, Biotek, Winooski, Vermont, United States) using ThT fluorimetric assay. The excitation and emission wavelengths were set at 440/30 and 485/20 nm, respectively. Inhibition experiments were monitored by incubating Aβ_{1-42} at the given conditions in the presence or absence of the tested compound. Doxycycline and methylene blue (50 μM) were used as reference inhibitors; parent compounds tacrine e PHT were also evaluated. Fluorescence emission was recorded every 10 min during 72 h incubation time without any stirring. Each inhibitor was assayed in duplicate in two independent experiments. The presented values were averaged and are expressed as the mean ± SEM (the standard error of the mean). The ratio according to eq 1 was calculated after subtraction of fluorescence of unbound ThT

$$R = \frac{F_{\text{plateau}} - F_{\text{lag}}}{F_{\text{lag}}} \quad (1)$$

where F_{lag} and F_{plateau} are fluorescence intensities of Aβ_{1-42} in lag and plateau phases of the aggregation kinetic at five time points every 30 min, respectively. After that, the percent inhibition of Aβ_{1-42} aggregation was calculated as follows (eq 2):

$$\%\ \text{inhibition} = 100 - \left(\frac{R_I}{R_0}\right) \times 100 \quad (2)$$

where R_I and R_0 are ratios according to eq 1 with or without studied compounds, respectively.

■ ASSOCIATED CONTENT

Supporting Information

The Supporting Information is available free of charge at https://pubs.acs.org/doi/10.1021/acschemneuro.1c00184.

Chemical synthesis of linker precursors **3**, **4**, and **6**; NMR, LC-MS, and HRMS spectra of final products; antioxidant properties; cholinesterase activity; MTT and MDCK assays; and design of *in vivo* studies (PDF)

■ AUTHOR INFORMATION

Corresponding Authors

Jan Korabecny − *Biomedical Research Centre, University Hospital Hradec Kralove, 500 05 Hradec Kralove, Czech Republic; Department of Toxicology and Military Pharmacy, Faculty of Military Health Sciences, University of Defense, 500 01 Hradec Kralove, Czech Republic;* orcid.org/0000-0001-6977-7596; Email: jan.korabecny@fnhk.cz

Maria Laura Bolognesi − *Department of Pharmacy and Biotechnology, University of Bologna, 40126 Bologna, Italy;* orcid.org/0000-0002-1289-5361; Email: marialaura.bolognesi@unibo.it

Authors

Lukas Gorecki − *Biomedical Research Centre, University Hospital Hradec Kralove, 500 05 Hradec Kralove, Czech Republic; Department of Toxicology and Military Pharmacy, Faculty of Military Health Sciences, University of Defense, 500 01 Hradec Kralove, Czech Republic; Department of*

https://doi.org/10.1021/acschemneuro.1c00184
ACS Chem. Neurosci. 2021, 12, 1698−1715

Pharmacy and Biotechnology, University of Bologna, 40126 Bologna, Italy; orcid.org/0000-0002-4791-6556

Elisa Uliassi − *Department of Pharmacy and Biotechnology, University of Bologna, 40126 Bologna, Italy;* orcid.org/0000-0002-0990-2532

Manuela Bartolini − *Department of Pharmacy and Biotechnology, University of Bologna, 40126 Bologna, Italy;* orcid.org/0000-0002-2890-3856

Jana Janockova − *Biomedical Research Centre, University Hospital Hradec Kralove, 500 05 Hradec Kralove, Czech Republic*

Martina Hrabinova − *Biomedical Research Centre, University Hospital Hradec Kralove, 500 05 Hradec Kralove, Czech Republic; Department of Toxicology and Military Pharmacy, Faculty of Military Health Sciences, University of Defense, 500 01 Hradec Kralove, Czech Republic*

Vendula Hepnarova − *Biomedical Research Centre, University Hospital Hradec Kralove, 500 05 Hradec Kralove, Czech Republic; Department of Toxicology and Military Pharmacy, Faculty of Military Health Sciences, University of Defense, 500 01 Hradec Kralove, Czech Republic*

Lukas Prchal − *Biomedical Research Centre, University Hospital Hradec Kralove, 500 05 Hradec Kralove, Czech Republic*

Lubica Muckova − *Biomedical Research Centre, University Hospital Hradec Kralove, 500 05 Hradec Kralove, Czech Republic; Department of Toxicology and Military Pharmacy, Faculty of Military Health Sciences, University of Defense, 500 01 Hradec Kralove, Czech Republic*

Jaroslav Pejchal − *Department of Toxicology and Military Pharmacy, Faculty of Military Health Sciences, University of Defense, 500 01 Hradec Kralove, Czech Republic*

Jana Z. Karasova − *Biomedical Research Centre, University Hospital Hradec Kralove, 500 05 Hradec Kralove, Czech Republic; Department of Toxicology and Military Pharmacy, Faculty of Military Health Sciences, University of Defense, 500 01 Hradec Kralove, Czech Republic*

Eva Mezeiova − *Biomedical Research Centre, University Hospital Hradec Kralove, 500 05 Hradec Kralove, Czech Republic*

Marketa Benkova − *Biomedical Research Centre, University Hospital Hradec Kralove, 500 05 Hradec Kralove, Czech Republic*

Tereza Kobrlova − *Biomedical Research Centre, University Hospital Hradec Kralove, 500 05 Hradec Kralove, Czech Republic; Department of Toxicology and Military Pharmacy, Faculty of Military Health Sciences, University of Defense, 500 01 Hradec Kralove, Czech Republic*

Ondrej Soukup − *Biomedical Research Centre, University Hospital Hradec Kralove, 500 05 Hradec Kralove, Czech Republic;* orcid.org/0000-0001-6376-8701

Sabrina Petralla − *Department of Pharmacy and Biotechnology, University of Bologna, 40126 Bologna, Italy*

Barbara Monti − *Department of Pharmacy and Biotechnology, University of Bologna, 40126 Bologna, Italy;* orcid.org/0000-0003-0330-482X

Complete contact information is available at: https://pubs.acs.org/10.1021/acschemneuro.1c00184

Author Contributions

L.G. and E.U. handled chemical synthesis and manuscript writing. E.M. handled chemical synthesis. M.B. handled anti-τ properties and manuscript writing. J.J. handled anti-τ properties. M.H. and V.H. handled anticholinesterase activity and DPPH. L.P. handled HRMS, LC-MS, and *in vivo* analysis. L.M. handled HepG2 cytotoxicity. J.P. and J.Z.K. handled *in vivo* studies. T.K. and O.S. handled the *in vitro* BBB permeation assay. S.P. and B.M. handled the neurotoxicity assay. J.K. and M.L.B. handled the manuscript writing and experiment supervision.

Notes

The authors declare no competing financial interest.

■ ACKNOWLEDGMENTS

The study was supported by a grant from the Ministry of Defence "Long Term Development Plan" Medical Aspects of Weapons of Mass Destruction of the Faculty of Military Health Sciences, University of Defence; by the Ministry of Education, Youth and Sports of Czech Republic (project ERDF no. CZ.02.1.01/0.0/0.0/18_069/0010054); and by the Grant from the Czech Science Foundation (20-29633J). Marvin was used for drawing, displaying, and characterizing chemical structures, substructures, and reactions (Marvin 17.21.0, ChemAxon, https://www.chemaxon.com). The abroad internship for LG was supported by the Faculty of Military Health Sciences, University of Defence (Czech Republic, Long-term development plan). M.L.B. and M.B. would also like to acknowledge the University of Bologna and the Italian Ministry for Education, Universities and Research (MIUR), for the financial support.

■ REFERENCES

(1) Cavalli, A., Bolognesi, M. L., Minarini, A., Rosini, M., Tumiatti, V., Recanatini, M., and Melchiorre, C. (2008) Multi-Target-Directed Ligands To Combat Neurodegenerative Diseases. *J. Med. Chem. 51* (3), 347−372.

(2) de Freitas Silva, M., Dias, K. S. T., Gontijo, V. S., Ortiz, C. J. C., and Viegas, C. (2018) Multi-Target Directed Drugs as a Modern Approach for Drug Design Towards Alzheimer's Disease: An Update. *Curr. Med. Chem. 25* (29), 3491−3525.

(3) Dias, K. S. T., and Viegas, C. (2014) Multi-Target Directed Drugs: A Modern Approach for Design of New Drugs for the Treatment of Alzheimer's Disease. *Curr. Neuropharmacol. 12* (3), 239−255.

(4) Oset-Gasque, M. J., and Marco-Contelles, J. (2018) Alzheimer's Disease, the "One-Molecule, One-Target" Paradigm, and the Multitarget Directed Ligand Approach. *ACS Chem. Neurosci. 9* (3), 401−403.

(5) Prati, F., Cavalli, A., and Bolognesi, M. L. (2016) Navigating the Chemical Space of Multitarget-Directed Ligands: From Hybrids to Fragments in Alzheimer's Disease. *Molecules 21* (4), 466.

(6) Zhou, J., Jiang, X., He, S., Jiang, H., Feng, F., Liu, W., Qu, W., and Sun, H. (2019) Rational Design of Multitarget-Directed Ligands: Strategies and Emerging Paradigms. *J. Med. Chem. 62*, 8881.

(7) Benek, O., Korabecny, J., and Soukup, O. (2020) A Perspective on Multi-Target Drugs for Alzheimer's Disease. *Trends Pharmacol. Sci. 41* (7), 434−445.

(8) Galimberti, D., and Scarpini, E. (2016) Old and New Acetylcholinesterase Inhibitors for Alzheimer's Disease. *Expert Opin. Invest. Drugs 25* (10), 1181−1187.

(9) Zemek, F., Drtinova, L., Nepovimova, E., Sepsova, V., Korabecny, J., Klimes, J., and Kuca, K. (2014) Outcomes of Alzheimer's Disease Therapy with Acetylcholinesterase Inhibitors and Memantine. *Expert Opin. Drug Saf. 13* (6), 759−774.

(10) Hardy, J. A., and Higgins, G. A. (1992) Alzheimer's Disease: The Amyloid Cascade Hypothesis. *Science 256* (5054), 184−185.

(11) Selkoe, D. J., and Hardy, J. (2016) The Amyloid Hypothesis of Alzheimer's Disease at 25 Years. *EMBO Mol. Med. 8* (6), 595−608.

(12) Villemagne, V. L., Fodero-Tavoletti, M. T., Masters, C. L., and Rowe, C. C. (2015) Tau Imaging: Early Progress and Future Directions. *Lancet Neurol. 14* (1), 114−124.
(13) Ballatore, C., Lee, V. M.-Y., and Trojanowski, J. Q. (2007) Tau-Mediated Neurodegeneration in Alzheimer's Disease and Related Disorders. *Nat. Rev. Neurosci. 8* (9), 663−672.
(14) Gandini, A., Bartolini, M., Tedesco, D., Martinez-Gonzalez, L., Roca, C., Campillo, N. E., Zaldivar-Diez, J., Perez, C., Zuccheri, G., Miti, A., et al. (2018) Tau-Centric Multitarget Approach for Alzheimer's Disease: Development of First-in-Class Dual Glycogen Synthase Kinase 3β and Tau-Aggregation Inhibitors. *J. Med. Chem. 61* (17), 7640−7656.
(15) Prati, F., De Simone, A., Bisignano, P., Armirotti, A., Summa, M., Pizzirani, D., Scarpelli, R., Perez, D. I., Andrisano, V., Perez-Castillo, A., et al. (2015) Multitarget Drug Discovery for Alzheimer's Disease: Triazinones as BACE-1 and GSK-3β Inhibitors. *Angew. Chem., Int. Ed. 54* (5), 1578−1582.
(16) Horak, M., Holubova, K., Nepovimova, E., Krusek, J., Kaniakova, M., Korabecny, J., Vyklicky, L., Kuca, K., Stuchlik, A., Ricny, J., et al. (2017) The Pharmacology of Tacrine at N-Methyl-d-Aspartate Receptors. *Prog. Neuro-Psychopharmacol. Biol. Psychiatry 75*, 54−62.
(17) Praticò, D. (2008) Evidence of Oxidative Stress in Alzheimer's Disease Brain and Antioxidant Therapy: Lights and Shadows. *Ann. N. Y. Acad. Sci. 1147*, 70−78.
(18) Sharma, A., Pachauri, V., and Flora, S. J. S. (2018) Advances in Multi-Functional Ligands and the Need for Metal-Related Pharmacology for the Management of Alzheimer Disease. *Front. Pharmacol. 9*, 1247.
(19) Wang, H., and Zhang, H. (2019) Reconsideration of Anticholinesterase Therapeutic Strategies against Alzheimer's Disease. *ACS Chem. Neurosci. 10* (2), 852−862.
(20) Nepovimova, E., Uliassi, E., Korabecny, J., Peña-Altamira, L. E., Samez, S., Pesaresi, A., Garcia, G. E., Bartolini, M., Andrisano, V., Bergamini, C., et al. (2014) Multitarget Drug Design Strategy: Quinone-Tacrine Hybrids Designed to Block Amyloid-β Aggregation and to Exert Anticholinesterase and Antioxidant Effects. *J. Med. Chem. 57* (20), 8576−8589.
(21) Giacobini, E. (1998) Invited Review: Cholinesterase Inhibitors for Alzheimer's Disease Therapy: From Tacrine to Future Applications. *Neurochem. Int. 32* (5−6), 413−419.
(22) Recanatini, M., Cavalli, A., Belluti, F., Piazzi, L., Rampa, A., Bisi, A., Gobbi, S., Valenti, P., Andrisano, V., Bartolini, M., et al. (2000) SAR of 9-Amino-1,2,3,4-Tetrahydroacridine-Based Acetylcholinesterase Inhibitors: Synthesis, Enzyme Inhibitory Activity, QSAR, and Structure-Based CoMFA of Tacrine Analogues. *J. Med. Chem. 43* (10), 2007−2018.
(23) Soukup, O., Jun, D., Zdarova-Karasova, J., Patocka, J., Musilek, K., Korabecny, J., Krusek, J., Kaniakova, M., Sepsova, V., Mandikova, J., et al. (2013) A Resurrection of 7-MEOTA: A Comparison with Tacrine. *Curr. Alzheimer Res. 10* (8), 893−906.
(24) Ohlow, M. J., and Moosmann, B. (2011) Phenothiazine: The Seven Lives of Pharmacology's First Lead Structure. *Drug Discovery Today 16* (3−4), 119−131.
(25) Mitchell, S. C. (2006) Phenothiazine: The Parent Molecule. *Curr. Drug Targets 7* (9), 1181−1189.
(26) WHO, *The Selection and Use of Essential Medicines*. http://www.who.int/medicines/publications/essentialmedicines/trs-1006-2017/en/ (accessed 2019-01-08).
(27) Wu, J., Li, A., Li, Y., Li, X., Zhang, Q., Song, W., Wang, Y., Ogutu, J. O., Wang, J., Li, J., et al. (2016) Chlorpromazine Inhibits Mitochondrial Apoptotic Pathway via Increasing Expression of Tissue Factor. *Int. J. Biochem. Cell Biol. 70*, 82−91.
(28) Li, H.-J., Zhang, Y.-J., Zhou, L., Han, F., Wang, M.-Y., Xue, M.-Q., and Qi, Z. (2014) Chlorpromazine Confers Neuroprotection against Brain Ischemia by Activating BKCa Channel. *Eur. J. Pharmacol. 735*, 38−43.
(29) Murphy, C. M., Ravner, H., and Smith, N. L. (1950) Mode of Action of Phenothiazine-Type Antioxidants. *Ind. Eng. Chem. 42* (12), 2479−2489.
(30) Tin, G., Mohamed, T., Gondora, N., Beazely, M. A., and Rao, P. P. N. (2015) Tricyclic Phenothiazine and Phenoselenazine Derivatives as Potential Multi-Targeting Agents to Treat Alzheimer's Disease. *MedChemComm 6* (11), 1930−1941.
(31) Uliassi, E., Peña-Altamira, L. E., Morales, A. V., Massenzio, F., Petralla, S., Rossi, M., Roberti, M., Martinez Gonzalez, L., Martinez, A., Monti, B., et al. (2019) A Focused Library of Psychotropic Analogues with Neuroprotective and Neuroregenerative Potential. *ACS Chem. Neurosci. 10* (1), 279−294.
(32) Darvesh, S., McDonald, R. S., Penwell, A., Conrad, S., Darvesh, K. V., Mataija, D., Gomez, G., Caines, A., Walsh, R., and Martin, E. (2005) Structure-Activity Relationships for Inhibition of Human Cholinesterases by Alkyl Amide Phenothiazine Derivatives. *Bioorg. Med. Chem. 13* (1), 211−222.
(33) González-Muñoz, G. C., Arce, M. P., López, B., Pérez, C., Villarroya, M., López, M. G., García, A. G., Conde, S., and Rodríguez-Franco, M. I. (2010) Old Phenothiazine and Dibenzothiadiazepine Derivatives for Tomorrow's Neuroprotective Therapies against Neurodegenerative Diseases. *Eur. J. Med. Chem. 45* (12), 6152−6158.
(34) Taniguchi, S., Suzuki, N., Masuda, M., Hisanaga, S., Iwatsubo, T., Goedert, M., and Hasegawa, M. (2005) Inhibition of Heparin-Induced Tau Filament Formation by Phenothiazines, Polyphenols, and Porphyrins. *J. Biol. Chem. 280* (9), 7614−7623.
(35) Jia, Q., Deng, Y., and Qing, H. (2014) Potential Therapeutic Strategies for Alzheimer's Disease Targeting or Beyond β-Amyloid: Insights from Clinical Trials. *BioMed Res. Int. 2014*, 1.
(36) Stack, C., Jainuddin, S., Elipenahli, C., Gerges, M., Starkova, N., Starkov, A. A., Jové, M., Portero-Otin, M., Launay, N., Pujol, A., et al. (2014) Methylene Blue Upregulates Nrf2/ARE Genes and Prevents Tau-Related Neurotoxicity. *Hum. Mol. Genet. 23* (14), 3716−3732.
(37) *Cognitive and Functional Connectivity Effects of Methylene Blue in Healthy Aging, Mild Cognitive Impairment and Alzheimer's Disease*, https://clinicaltrials.gov/ct2/show/NCT02380573 (accessed 2019-01-08).
(38) Wilcock, G. K., Gauthier, S., Frisoni, G. B., Jia, J., Hardlund, J. H., Moebius, H. J., Bentham, P., Kook, K. A., Schelter, B. O., Wischik, D. J., et al. (2017) Potential of Low Dose Leuco-Methylthioninium Bis(Hydromethanesulphonate) (LMTM) Monotherapy for Treatment of Mild Alzheimer's Disease: Cohort Analysis as Modified Primary Outcome in a Phase III Clinical Trial. *J. Alzheimer's Dis. 61* (1), 435−457.
(39) Lexchin, J. (2012) Sponsorship Bias in Clinical Research. *Int. J. Risk Saf. Med. 24* (4), 233−242.
(40) Hui, A., Chen, Y., Zhu, S., Gan, C., Pan, J., and Zhou, A. (2014) Design and Synthesis of Tacrine-Phenothiazine Hybrids as Multi-target Drugs for Alzheimer's Disease. *Med. Chem. Res. 23* (7), 3546−3557.
(41) Rydberg, E. H., Brumshtein, B., Greenblatt, H. M., Wong, D. M., Shaya, D., Williams, L. D., Carlier, P. R., Pang, Y.-P., Silman, I., and Sussman, J. L. (2006) Complexes of Alkylene-Linked Tacrine Dimers with Torpedo Californica Acetylcholinesterase: Binding of Bis5-Tacrine Produces a Dramatic Rearrangement in the Active-Site Gorge. *J. Med. Chem. 49* (18), 5491−5500.
(42) Camps, P., Formosa, X., Galdeano, C., Gómez, T., Muñoz-Torrero, D., Ramírez, L., Viayna, E., Gómez, E., Isambert, N., Lavilla, R., et al. (2010) Tacrine-Based Dual Binding Site Acetylcholinesterase Inhibitors as Potential Disease-Modifying Anti-Alzheimer Drug Candidates. *Chem.-Biol. Interact. 187* (1−3), 411−415.
(43) Carlier, P. R., Han, Y. F., Chow, E. S., Li, C. P., Wang, H., Lieu, T. X., Wong, H. S., and Pang, Y. P. (1999) Evaluation of Short-Tether Bis-THA AChE Inhibitors. A Further Test of the Dual Binding Site Hypothesis. *Bioorg. Med. Chem. 7* (2), 351−357.
(44) Uliassi, E. (2016) Towards the Development of Chemical Biology Pipelines for Stem Cells and Receptor Characterization. Dissertation thesis, Alma Mater Studiorum Università di Bologna, DOI: 10.6092/unibo/amsdottorato/7656.

(45) Jackson, D. S., Fraser, S. A., Ni, L.-M., Kam, C.-M., Winkler, U., Johnson, D. A., Froelich, C. J., Hudig, D., and Powers, J. C. (1998) Synthesis and Evaluation of Diphenyl Phosphonate Esters as Inhibitors of the Trypsin-like Granzymes A and K and Mast Cell Tryptase. *J. Med. Chem. 41* (13), 2289−2301.
(46) Righi, M., Bedini, A., Piersanti, G., Romagnoli, F., and Spadoni, G. (2011) Direct, One-Pot Reductive Alkylation of Anilines with Functionalized Acetals Mediated by Triethylsilane and TFA. Straightforward Route for Unsymmetrically Substituted Ethylenediamine. *J. Org. Chem. 76* (2), 704−707.
(47) Staderini, M., Cabezas, N., Bolognesi, M. L., and Menéndez, J. C. (2013) Solvent- and Chromatography-Free Amination of π-Deficient Nitrogen Heterocycles under Microwave Irradiation. A Fast, Efficient and Green Route to 9-Aminoacridines, 4-Aminoquinolines and 4-Aminoquinazolines and Its Application to the Synthesis of the Drugs Amsacrine and Bistacrine. *Tetrahedron 69* (3), 1024−1030.
(48) Ellman, G. L., Courtney, K. D., Andres, V., and Feather-Stone, R. M. (1961) A New and Rapid Colorimetric Determination of Acetylcholinesterase Activity. *Biochem. Pharmacol. 7*, 88−95.
(49) Nepovimova, E., Korabecny, J., Dolezal, R., Babkova, K., Ondrejicek, A., Jun, D., Sepsova, V., Horova, A., Hrabinova, M., Soukup, O., et al. (2015) Tacrine-Trolox Hybrids: A Novel Class of Centrally Active, Nonhepatotoxic Multi-Target-Directed Ligands Exerting Anticholinesterase and Antioxidant Activities with Low In Vivo Toxicity. *J. Med. Chem. 58* (22), 8985−9003.
(50) Lockridge, O. (2015) Review of Human Butyrylcholinesterase Structure, Function, Genetic Variants, History of Use in the Clinic, and Potential Therapeutic Uses. *Pharmacol. Ther. 148*, 34−46.
(51) Franjesevic, A. J., Sillart, S. B., Beck, J. M., Vyas, S., Callam, C. S., and Hadad, C. M. (2019) Resurrection and Reactivation of Acetylcholinesterase and Butyrylcholinesterase. *Chem. - Eur. J. 25* (21), 5337−5371.
(52) Davies, P., and Maloney, A. J. (1976) Selective Loss of Central Cholinergic Neurons in Alzheimer's Disease. *Lancet London Engl. 2* (8000), 1403.
(53) Siek, G. C., Katz, L. S., Fishman, E. B., Korosi, T. S., and Marquis, J. K. (1990) Molecular Forms of Acetylcholinesterase in Subcortical Areas of Normal and Alzheimer Disease Brain. *Biol. Psychiatry 27* (6), 573−580.
(54) Nordberg, A., Ballard, C., Bullock, R., Darreh-Shori, T., and Somogyi, M. (2013) A Review of Butyrylcholinesterase as a Therapeutic Target in the Treatment of Alzheimer's Disease. *Prim. Care Companion CNS Disord. 15* (2), 1 DOI: 10.4088/PCC.12r01412.
(55) Mesulam, M. M., and Geula, C. (1994) Butyrylcholinesterase Reactivity Differentiates the Amyloid Plaques of Aging from Those of Dementia. *Ann. Neurol. 36* (5), 722−727.
(56) Podoly, E., Shalev, D. E., Shenhar-Tsarfaty, S., Bennett, E. R., Ben Assayag, E., Wilgus, H., Livnah, O., and Soreq, H. (2009) The Butyrylcholinesterase K Variant Confers Structurally Derived Risks for Alzheimer Pathology. *J. Biol. Chem. 284* (25), 17170−17179.
(57) Diamant, S., Podoly, E., Friedler, A., Ligumsky, H., Livnah, O., and Soreq, H. (2006) Butyrylcholinesterase Attenuates Amyloid Fibril Formation in Vitro. *Proc. Natl. Acad. Sci. U. S. A. 103* (23), 8628−8633.
(58) Darvesh, S., Cash, M. K., Reid, G. A., Martin, E., Mitnitski, A., and Geula, C. (2012) Butyrylcholinesterase Is Associated with β-Amyloid Plaques in the Transgenic APPSWE/PSEN1dE9Mouse Model of Alzheimer Disease. *J. Neuropathol. Exp. Neurol. 71* (1), 2−14.
(59) Mosmann, T. (1983) Rapid Colorimetric Assay for Cellular Growth and Survival: Application to Proliferation and Cytotoxicity Assays. *J. Immunol. Methods 65* (1), 55−63.
(60) Hepnarova, V., Korabecny, J., Matouskova, L., Jost, P., Muckova, L., Hrabinova, M., Vykoukalova, N., Kerhartova, M., Kucera, T., Dolezal, R., et al. (2018) The Concept of Hybrid Molecules of Tacrine and Benzyl Quinolone Carboxylic Acid (BQCA) as Multifunctional Agents for Alzheimer's Disease. *Eur. J. Med. Chem. 150*, 292−306.
(61) Dgachi, Y., Martin, H., Bonet, A., Chioua, M., Iriepa, I., Moraleda, I., Chabchoub, F., Marco-Contelles, J., and Ismaili, L. (2017) Synthesis and Biological Assessment of Racemic Benzochromenopyrimidinetriones as Promising Agents for Alzheimer's Disease Therapy. *Future Med. Chem. 9* (8), 715−721.
(62) Watkins, P. B., Zimmerman, H. J., Knapp, M. J., Gracon, S. I., and Lewis, K. W. (1994) Hepatotoxic Effects of Tacrine Administration in Patients with Alzheimer's Disease. *JAMA 271* (13), 992−998.
(63) Molyneux, P. (2004) Use of the Stable Free Radical Diphenylpicryl- Hydrazyl (DPPH) for Estimating Antioxidant Activity. *SJST 26* (2), 9.
(64) Gorecki, L., Junova, L., Kucera, T., Hepnarova, V., Prchal, L., Kobrlova, T., Muckova, L., Soukup, O., and Korabecny, J. (2019) Tacroximes: Novel Unique Compounds for the Recovery of Organophosphorus-Inhibited Acetylcholinesterase. *Future Med. Chem. 11* (20), 2625−2634.
(65) von Bergen, M., Friedhoff, P., Biernat, J., Heberle, J., Mandelkow, E. M., and Mandelkow, E. (2000) Assembly of Tau Protein into Alzheimer Paired Helical Filaments Depends on a Local Sequence Motif ((306)VQIVYK(311)) Forming Beta Structure. *Proc. Natl. Acad. Sci. U. S. A. 97* (10), 5129−5134.
(66) Stöhr, J., Wu, H., Nick, M., Wu, Y., Bhate, M., Condello, C., Johnson, N., Rodgers, J., Lemmin, T., Acharya, S., et al. (2017) A 31-Residue Peptide Induces Aggregation of Tau's Microtubule-Binding Region in Cells. *Nat. Chem. 9* (9), 874−881.
(67) Minoura, K., Tomoo, K., Ishida, T., Hasegawa, H., Sasaki, M., and Taniguchi, T. (2002) Amphipathic Helical Behavior of the Third Repeat Fragment in the Tau Microtubule-Binding Domain, Studied by 1H NMR Spectroscopy. *Biochem. Biophys. Res. Commun. 294* (2), 210−214.
(68) Gremer, L., Schölzel, D., Schenk, C., Reinartz, E., Labahn, J., Ravelli, R. B. G., Tusche, M., Lopez-Iglesias, C., Hoyer, W., Heise, H., et al. (2017) Fibril Structure of Amyloid-β(1−42) by Cryo−electron Microscopy. *Science 358* (6359), 116−119.
(69) Frydman-Marom, A., Rechter, M., Shefler, I., Bram, Y., Shalev, D. E., and Gazit, E. (2009) Cognitive-Performance Recovery of Alzheimer's Disease Model Mice by Modulation of Early Soluble Amyloidal Assemblies. *Angew. Chem., Int. Ed. 48* (11), 1981−1986.
(70) Gazit, E. (2002) A Possible Role for π-Stacking in the Self-Assembly of Amyloid Fibrils. *FASEB J. 16* (1), 77−83.
(71) Budyak, I. L., Zhuravleva, A., and Gierasch, L. M. (2013) The Role of Aromatic-Aromatic Interactions in Strand-Strand Stabilization of β-Sheets. *J. Mol. Biol. 425* (18), 3522−3535.
(72) Bartolini, M., Bertucci, C., Bolognesi, M. L., Cavalli, A., Melchiorre, C., and Andrisano, V. (2007) Insight Into the Kinetic of Amyloid β (1−42) Peptide Self-Aggregation: Elucidation of Inhibitors' Mechanism of Action. *ChemBioChem 8* (17), 2152−2161.
(73) Chalupova, K., Korabecny, J., Bartolini, M., Monti, B., Lamba, D., Caliandro, R., Pesaresi, A., Brazzolotto, X., Gastellier, A.-J., Nachon, F., et al. (2019) Novel Tacrine-Tryptophan Hybrids: Multi-Target Directed Ligands as Potential Treatment for Alzheimer's Disease. *Eur. J. Med. Chem. 168*, 491−514.
(74) León, R., Garcia, A. G., and Marco-Contelles, J. (2013) Recent Advances in the Multitarget-Directed Ligands Approach for the Treatment of Alzheimer's Disease. *Med. Res. Rev. 33* (1), 139−189.
(75) Hamley, I. W. (2012) The Amyloid Beta Peptide: A Chemist's Perspective. Role in Alzheimer's and Fibrillization. *Chem. Rev. 112* (10), 5147−5192.
(76) Necula, M., Breydo, L., Milton, S., Kayed, R., van der Veer, W. E., Tone, P., and Glabe, C. G. (2007) Methylene Blue Inhibits Amyloid Aβ Oligomerization by Promoting Fibrillization. *Biochemistry 46* (30), 8850−8860.
(77) McNally, W. P., Pool, W. F., Sinz, M. W., Dehart, P., Ortwine, D. F., Huang, C. C., Chang, T., and Woolf, T. F. (1996) Distribution of Tacrine and Metabolites in Rat Brain and Plasma after Single- and Multiple-Dose Regimens. Evidence for Accumulation of Tacrine in Brain Tissue. *Drug Metab. Dispos. Biol. Fate Chem. 24* (6), 628−633.